Geological Magazine

www.cambridge.org/geo

The affinity of microcontinents in northern East Gondwana in the Silurian: Hainan Island response to the closure of the Proto-Tethys Ocean

Shiyao Gao[1], Zhongjie Xu[1,2], Jintao Kong[1], Hua Tan[1], Yingming sun[1], Hexue Fu[1] and Yin Ming[1]

[1]College of Earth Sciences, Jilin University, Changchun 130061, Jilin, China and [2]Key Laboratory of Mineral Resources Evaluation in Northeast Asia, Ministry of Natural and Resources, Changchun 130061, China

Original Article

Cite this article: Gao S, Xu Z, Kong J, Tan H, sun Y, Fu H, and Ming Y (2023) The affinity of microcontinents in northern East Gondwana in the Silurian: Hainan Island response to the closure of the Proto-Tethys Ocean. *Geological Magazine* **160**: 2110–2128. https://doi.org/10.1017/S0016756824000116

Received: 27 October 2023
Revised: 13 April 2024
Accepted: 14 April 2024
First published online: 14 May 2024

Keywords:
Hainan Island; early Silurian; zircon U-Pb dating; detrital zircon geochronology; Proto-Tethys Ocean closure

Corresponding author:
Zhongjie Xu; Email: zhongjiexu@jlu.edu.cn

Abstract

During the existence of Proto-Tethys Ocean (550–430 Ma), microcontinents in northern East Gondwana merged with the northern margin of India-Australia, completing the assembly of Gondwana. Ongoing controversy surrounds the disappearance of the Proto-Tethys Ocean, the dynamic mechanisms of suturing and the palaeogeographic relationships among microcontinents in northern East Gondwana, contributing to the uncertainty about the tectonic evolution of the region. This paper concerns the lower Silurian Zusailing Formation in the Hainan Island and focuses on the affinity between Hainan Island and various microcontinents in northern East Gondwana during the early Silurian. We use detrital zircon geochronology to reconstruct the closure process of the Proto-Tethys Ocean and show that the detrital zircon U–Pb age groups of the lower Silurian Zusailing Formation are 2800–2200, 2100–1350, 1250–950, 600–480 and 480–430 Ma, with a significant age peak of ca. 449 Ma. Furthermore, the analysis of detrital zircon geochemistry and europium anomalies shows that the Hainan Island crust continued to thicken during 600–434 Ma. Comparing the age spectrum of early Palaeozoic detrital zircons from Hainan Island and various microcontinents in northern East Gondwana, as well as the affinity among them during the Silurian, we conclude that the closure of the eastern Proto-Tethys Ocean evolved from unidirectional subduction (600–480 Ma) to bidirectional subduction (480–430 Ma).

1. Introduction

The tectonic evolution of the Tethys Ocean is a crucial stage in the evolution of the Earth, which can be divided into three stages: the Proto-Tethys stage (Cambrian–Silurian), the Palaeo-Tethys stage (Devonian–mid-Triassic) and the Neo-Tethys stage (since the Cretaceous) (Lu, 2004; Cawood *et al.* 2007; Sorkhabi & Heydari, 2008; Xu *et al.* 2012; Deng *et al.* 2016, 2019). The Proto-Tethys stage, which marks the incipient phase of the entire Tethys tectonic evolution, is crucial for understanding the history of the Gondwana. During the Proto-Tethys stage, various microcontinents in the northern East Gondwana (north of India and Australia) were gradually assembled, including the South China Block, Tarim Block, South Qiangtang Terranes, North Qiangtang Terranes, Indochina Block and Sibumasu Block (Fig. 1, Nie, 2016; Zhao, 2019; Zhang *et al.* 2022). According to palaeomagnetic, fossil and detrital zircon data during the early Palaeozoic, the South China Block, Tarim Block, North Qiangtang Terrane and Indochina Block were located close to each other. They are collectively referred to as the North Vietnam-South China and these microcontinents divide the Palaeo-Tethys Ocean into several narrow basins (Duan *et al.* 2011; McKenzie *et al.* 2011; Metcalfe, 2013; Xu *et al.* 2013; Zhou *et al.* 2015*a*; Chen *et al.* 2016; Lee *et al.* 2016; Han *et al.* 2016; Wang *et al.* 2016; Zhao *et al.* 2017, 2018; Liu, 2020; Wu *et al.* 2023). Therefore, the closure of the Proto-Tethys Ocean has stages, and its sutures are characterized by multiple zones, such as Truong Son, Changning–Menglian and Jinshajiang–Diancangshan–Ailaoshan structural zones (Fig. 1, Zhao, 2019; Zhou *et al.* 2021*a*, *b*; Peng *et al.* 2022).

Due to the lack of preserved records of late Palaeozoic magmatic activities near the original Tethys Ocean suture zone, as well as the thermal structural events associated with the closure of the ancient Tethys Ocean and the Himalayan Orogeny, the early Palaeozoic tectonic evolution and palaeogeographic positioning of the North Vietnam-South China with respect to the northern margin of India-Australia have not been well constrained. There are two dynamic models (the passive continental margin and the Andean-type active continental margin) to explain these events. The former is controlled by the break-up of the Rodinia supercontinent and the assembly of the Gondwana during the Pan-African Orogeny (Miller *et al.* 2001;

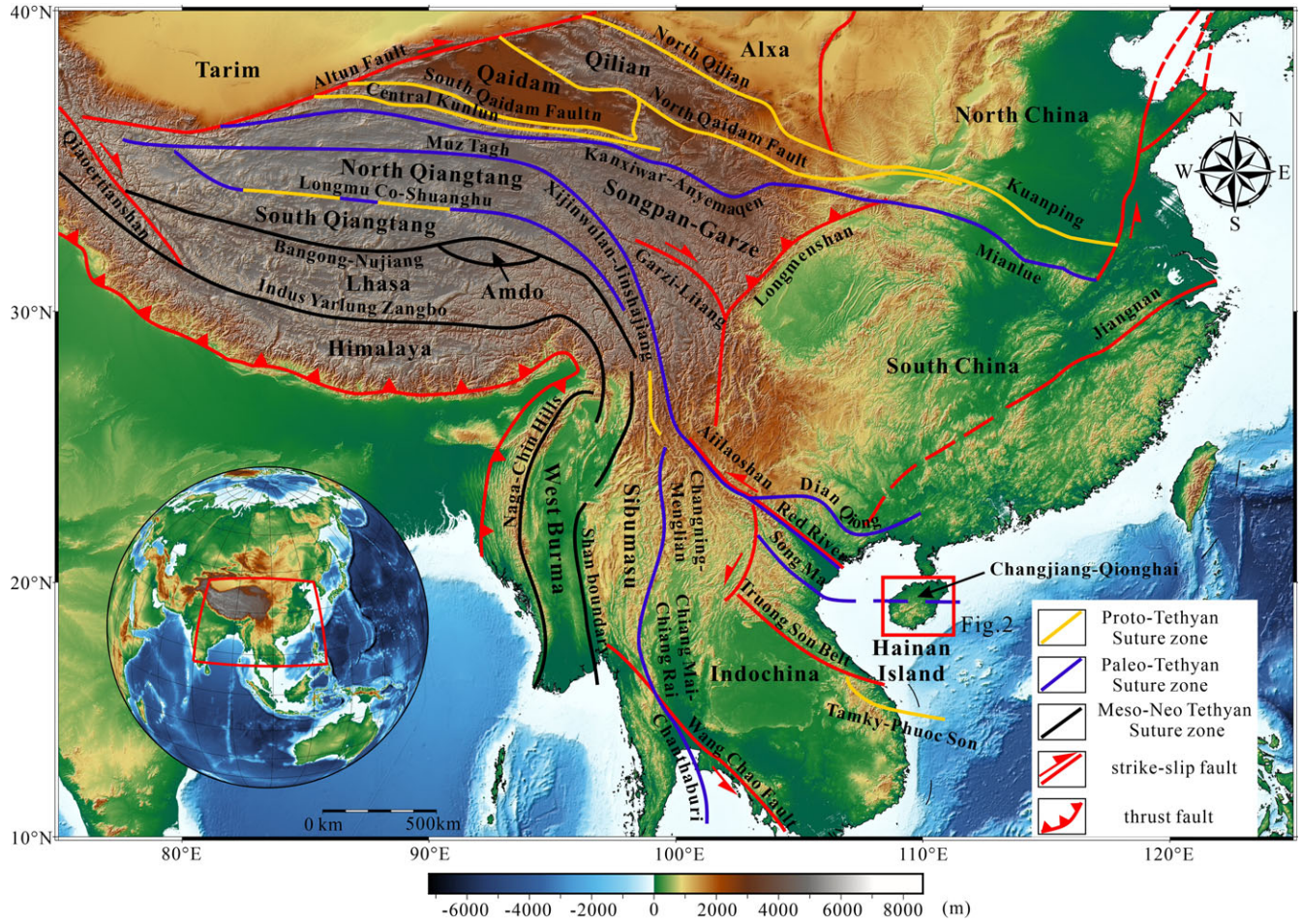

Figure 1. (Colour online) Schematic diagram of principal tectonic fragments and sutures in Southeast Asia (after Metcalfe, 2011, 2013, 2017).

Xu *et al.* 2005; Yang *et al.* 2012c; Cai *et al.* 2013; Liu *et al.* 2016). The latter is controlled by the subduction of the Proto-Tethys Ocean underneath Gondwana and adjacent microcontinents after the Pan-African Orogeny (Cawood *et al.* 2007; Dong *et al.* 2010; Zhu *et al.* 2012; Wang *et al.* 2013*a*; Li *et al.* 2016). In addition to the uncertainty of dynamic mechanisms, there is also controversy over the independence of, and affinity among, microcontinents in northern East Gondwana, including the reconstruction of the tectonic evolution and assembly of the microcontinents in the region during early Palaeozoic (north of India and Australia). Some believe that these microcontinents have an affinity with Gondwana (Dopieralska *et al.* 2012; Usuki *et al.* 2013; Burrett *et al.* 2014; Metcalfe, 2017), while others posit that they evolved as independent blocks in the Proto-Tethys Ocean and have the characteristics of the Pan-Cathaysian landmass groups (Zhang, 1994; Lu, 2001; Replumaz & Tapponnier, 2003; Zhang *et al.* 2005; Cocks & Torsvik, 2013).

During the early Silurian, Hainan Island was located in the northern region of East Gondwana (Cawood *et al.* 2007; Dong *et al.* 2010; Metcalfe, 2013; Xu *et al.* 2014; Zhou *et al.* 2015*a*). Due to the tectonic position of Hainan Island, the lower Silurian Zusailing Formation contains important information about the evolution of Proto-Tethys tectonics, which is an important clue to reveal the affinity between North Vietnam-South China and the northern margin of India-Australia. By studying the U-Pb ages of detrital zircons and geochemical data from the Zusailing Formation in early Silurian of Hainan Island, this article explores the tectonic events associated with Hainan Island during the late Early Palaeozoic. It reconstructs the main provenance areas during early Silurian and analyses the source-to-sink system, thereby determining the affinity among the various microcontinents in northern East Gondwana. These findings provide sedimentological evidence for the tectonic evolution stages of the early Palaeozoic in East Gondwana.

2. Geological setting and sample description

Hainan Island is located at the junction of the South China Block and the Indochina Block, which is located in the Palaeo-Tethys tectonic domain (Fig. 1) (Wen *et al.* 2013; Zhou *et al.* 2015*b*; Zhang *et al.* 2017; Li *et al.* 2018; Zhao *et al.* 2020; Gao *et al.* 2022*b*). The Hainan Island region experienced multiple periods and different forms of tectonic movements. The superposition of the effects of these tectonic movements has made the internal structural features of the Hainan Island complex. In the Mesoproterozoic-Neoproterozoic, the Jinning Orogeny formed the basement of Hainan Island. In the Palaeozoic, the Caledonian and Hercynian Orogeny laid the basic structural framework of Hainan Island, accompanied by large-scale magmatic activity and migmatization. In the Mesozoic, the Indosinian Orogeny mainly developed ductile deformation, controlling the eruption of a large number of intermediate to acidic magmas. The Cenozoic orogeny

https://doi.org/10.1017/S0016756824000116

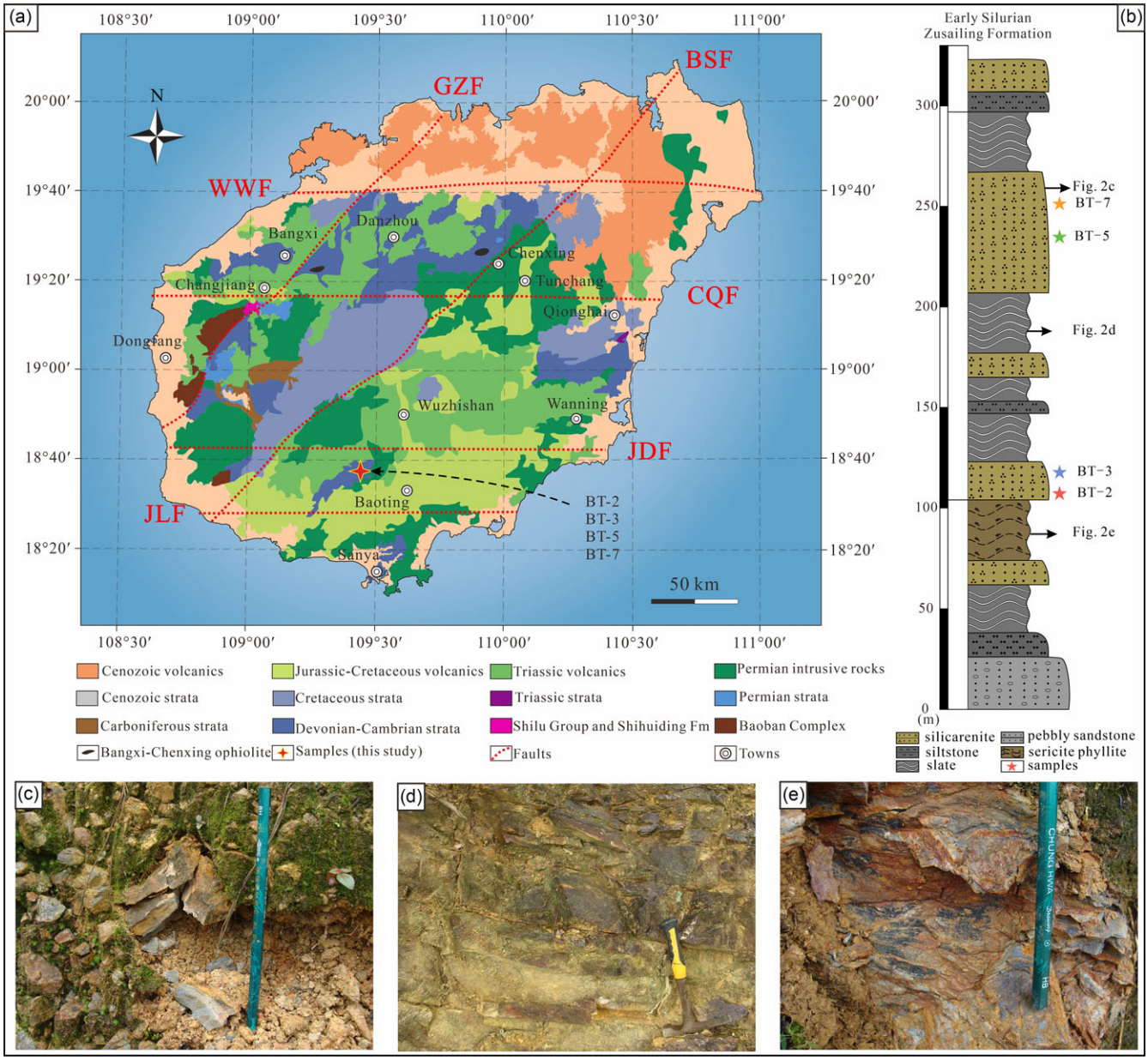

Figure 2. (Colour online) (a) Geological sketch of Hainan Island (according to the Bureau of Geology and Mineral Resources of Guangdong Province (BGMRGP) 1988; Gao *et al.* 2022b; Kong *et al.* 2022); GZF: Gezhen fault; BSF: Baisha fault; WWF: Wangwu-Wenjiao fault; CQF: Changjiang-Qionghai fault; JDF: Jianfeng-Diaoluo fault; JLF: Jiusuo-Lingshui fault; (b) Stratigraphic column of the lower Silurian Zusailing Formation; (c) sandstone representative photograph (The length of pencil is 17.5 cm); (d) slate representative photograph (The length of hammer is 30 cm); (e) sericite phyllite representative photograph (The length of pencil is 17.5 cm).

was dominated by fault block activity and large-scale basic magmatic eruption (Tang, 2010; Du *et al.* 2013; Zhou *et al.* 2015*b*; He *et al.* 2016; Yan *et al.* 2017; Wang *et al.* 2019). There are faults with a northeast trend in the region, from west to east the Gezhen and Baisha faults, and there are four nearly east-west oriented faults, namely the Wangwu–Wenjiao, Changjiang–Qionghai, Jianfeng–Diaoluo and Jiusuo–Lingshui faults from south to north (Fig. 2a) (Chao *et al.* 2016; Zhang *et al.* 2019; He *et al.* 2020; Liu *et al.* 2022*a*).

Existing research indicates that except for Jurassic rocks, strata from the Mesoproterozoic to the Quaternary system are exposed in Hainan Island, most of which are Palaeozoic (Wang *et al.* 1992). However, Palaeozoic rocks are in a fragmented state on Hainan Island, dispersed in different regions and with poor correlation between units. The early Palaeozoic strata are widely distributed in this area, mainly consisting of low-grade metamorphic, littoral to neritic facies sandstone and siltstone with carbonate rocks. Cambrian rocks are only preserved in the Sanya and Wanning areas, whereas Ordovician and Silurian rocks are widely distributed in Wanning and Qionghai in the east; Danzhou, Chengmai and Danzhou in the north; Changjiang in the west and Ledong and Nanhao in the south. Upper Palaeozoic rocks are mainly distributed in the north of the Jiusuo–Lingshui fault, including Devonian limestone, sandstone, siltstone and shale, as well as Carboniferous shales, metamorphic volcanic rocks and Permian limestone and sandstones (Hu *et al.* 2002; Long *et al.* 2007). This makes it extremely difficult to reconstruct Palaeozoic sedimentary environments and tectonic histories (Fig. 2a).

https://doi.org/10.1017/S0016756824000116

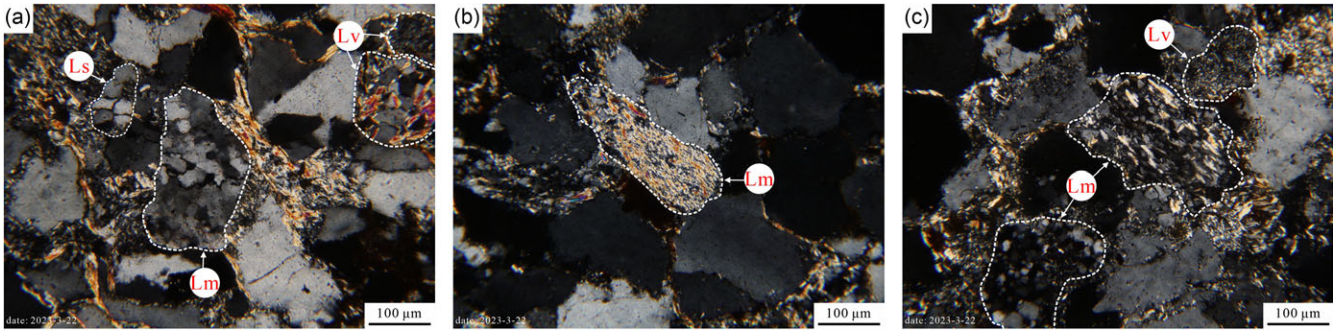

Figure 3. (Colour online) Photomicrographs of Lithic clasts (BT-4: medium-grained lithic quartz sandstone) (Lv: Volcanic rock fragments; Ls: Sedimentary rock fragments; Lm: Metamorphic rock fragments).

The Silurian strata in the Hainan Island are entirely lower Silurian, despite disputes over the ages of these rocks (Li *et al.* 2007, 2009; Chen *et al.* 2012; Zhang *et al.* 2013). The widely accepted stratigraphic framework is Kongliecun Formation (S_1k), Dagancun Formation (S_1d), Kaoqinshan Formation (S_1kq), Zusailing Formation (S_2z). Some Tetracoralla fossils, such as *Amplexoides* and *Tryplasma*, are present in the upper part of the limestone in the S_1k (Wang *et al.* 1992). The strata record changes in sea level, neritic sedimentation with abundant volcanic activity and the end of early Palaeozoic transgression in the Hainan Island (Yao *et al.* 1999). The S_1d is a set of clastic rocks and carbonate sedimentary deposits of a littoral–neritic shelf (Zeng *et al.* 2003, 2004). The S_1kq consists of fine siliciclastic rocks and carbonate rocks, with a rhythmic structure similar to flysch. It contains fossils such as *Nalivkinia*, *Xinanospirifer* and *Striispirifer*, indicating a sedimentary environment in the upper part of the subtidal zone (Zeng *et al.* 2003, 2004). Although the Zusailing Formation (S_2z) is rich in fossils, the fossil preservation is poor, indicating high-energy shallow water environment and the sedimentary facies evolved from neritic shelf to foreshore or nearshore facies (Li *et al.* 2007, 2009). The section is upwards coarsening from S_1kq to the lower part of Zusailing Formation, reflecting regression. There is evidence of an intracontinental orogeny in the early Palaeozoic of South China. The strong folding and deformation of the pre-Devonian system caused an angular unconformity below the overlying strata. This tectonic event also produced widespread magmatism and resulted in the formation of the Wuyi–Yunkai Orogen (Faure *et al.* 2009; Liu *et al.* 2010*a*; Charvet, 2013; Zhang *et al.* 2015). Therefore, the study area recorded an unconformity contact between top of Silurian Zusailing Formation and the Middle Devonian (Zhao *et al.* 2020; Yao *et al.* 2021), which marks the end of marine sedimentation and the beginning of long-term weathering and erosion in Hainan Island.

The lower Silurian Zusailing Formation studied in this paper is exposed in the Nanbing–Nanhao Highway section of Baoting County (109°27′58″, 18°36′24″). It is a set of clastic rocks formed in littoral to neritic shelf environments (Fig. 2b), and it mainly consists of sandstone, siltstone, slate, and greywacke rocks (Fig. 2c-e). The lower part consists of grey-yellow quartz sandstone and siltstone that were deposited in the littoral environment. There is also grey-black thin-layered slate and yellow-black, thin-layered sericite phyllite with black carbonaceous grains (Fig. 2b). The upper part mainly consists of greyish-yellow thin-layered siltstone that was deposited in the neritic environment, as well as medium-grained, yellowish-brown, quartz sandstone in thin to medium beds and slate in the middle to upper part (Fig. 2b), which has undergone sericitization. The group yield a large number of fossils, including brachiopods (*Xinanospirifer flabellum*, *Xinanospirifer* cf. *amanuensis*, *Xinanospirifer* sp., *Rhynchonellida* gen. sp. indet. *Spirifeda* gen. sp. indet), corals (*Favocites* sp. *Tetracoralla gen*. sp. indet.), trilobites (*Latiproetus* cf. *latilimbatus*), gastropods (*Homotoma* sp.), Sinacanthus (*Sinacanthus wuchangensis*) and fragmented crinoid fossils (*Pentagonocyclicus* sp., *Cyclocyclicus* sp.) (Li *et al.* 2009; Zhang *et al.* 2013).

We collected four samples BT-2, BT-3, BT-5 and BT-7 of medium-grained lithic quartz sandstone in the upper part of the section on the Nanbing–Nanhao Highway in Baoting County. The lithological characteristics of the samples are similar, all being sediments of the neritic shelf origin. Photomicrographs of the samples reveal some degree of alteration (sericitization), a medium-grained sandy texture, argillaceous cement and pore cementation, with a content of debris (87–90%) and interstitial fillings (10–13%). The grain size of the detrital particles ranges from 0.05mm to 0.5mm, and it is concentrated in 0.2 mm to 0.3 mm. The detrital particles are mostly granular, moderately sorted and subangular. The sandstone grains are mostly quartz (about 75%), with hypidiomorphic texture predominantly in the form of single crystal quartz, with a small amount of polycrystalline quartz and flint. The single crystal quartz exhibits undulose extinction. Lithic clasts (about 20%), include felsic volcanic rock, quartz sandstone, quartzite and schist (Fig. 3). Feldspar makes up about 5% of the grains, and these have undergone complete sericite alteration, with only pseudomorphs remaining. The interstitial fillings are mainly clay and calcareous mixed detrital constituents, and almost all of them have undergone sericite alteration. Sericite is identified as an interstitial phase, which is a scale aggregate with bright interference colour. Despite the weathering of the samples due to the hot and humid modern climate, the original rocks are identified as medium-grained lithic-rich quartz sandstones.

3. Analytical methods

Hebei Langfang Yuneng Mineral Sorting Company was responsible for the crushing treatment of samples. Zircon grains were separated from clastic rocks through heavy liquid and magnetic mineral separation techniques and hand-picked under a binocular microscope. Cathodoluminescence (CL) images were taken by Gantan MiniCL imaging system attached to a JSM-IT100 tungsten filament scanning electron microscope. Zircon U–Pb geochronology was carried out by Laser Ablation-Inductively Coupled Plasma-mass spectrometer (LA-ICP-MS) at the Key Laboratory of Mineral Resources Evaluation in Northeast Asia, Ministry of Land and Resources, Jilin University, Changchun, China. The GeoLasPro 193 nm ArF excimer laser by COMPExPro

https://doi.org/10.1017/S0016756824000116

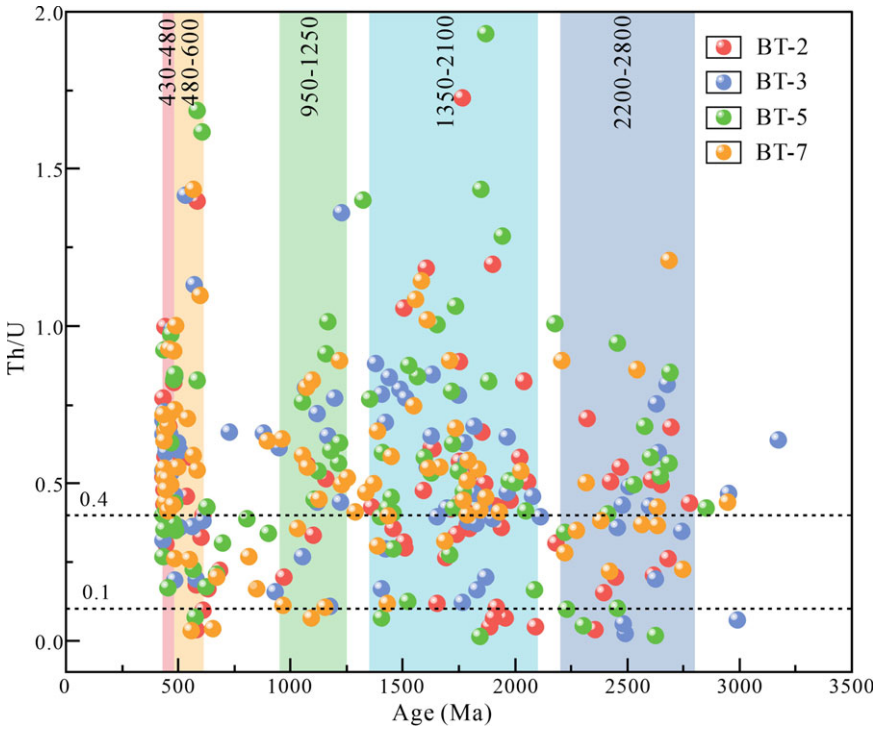

Figure 4. (Colour online) Th/U ratio–ages diagrams of detrital zircon analyses.

in Germany was used for laser ablation. The laser beam diameter was 32 μm, the laser fluence of 10 J/cm^2 and repetition rate of 8 Hz. The ICP-MS instrument used was an Agilent 7900. High-purity helium was used as carrier gas to provide efficient aerosol transport to the ICP and minimize aerosol deposition around the ablation site and within the transport tube with a gas flow of 600 mL/min. Argon was used as make-up gas with a gas flow of 1.15 L/min. The standard used was reference material NIST 610 (Liu *et al.* 2010), an artificial synthetic silicate glass developed by the National Institute of Standards and Technology (NIST) in the United States. The collection time for ^{49}Ti, ^{206}Pb and ^{208}Pb was 20 ms, for ^{207}Pb 30 ms, for ^{232}Th and ^{238}U 15 ms, and for other elements, it was 6 ms. Isotope ratio correction used the standard zircon 91500 (1062 Ma) as the primary reference material and 91500 was ablated every five unknowns (Wiedenbeck *et al.* 1995). Uranium, Th and Pb concentrations were calibrated using ^{29}Si as an internal standard. Glitter (ver4.0, Macquarie University) was used to calculate isotope ratio and age values of ^{207}Pb/^{206}Pb, ^{206}Pb/^{238}U and ^{207}Pb/^{235}U. Uncertainties of individual analyses are reported with 2s error. Concordance is calculated as: age >1000Ma (^{207}Pb/^{206}U age)/ (^{206}Pb/^{238}U age) × 100 (%); age<1000Ma, (^{207}Pb/^{235}U age)/ (^{206}Pb/^{238}U age) × 100 (%). Only analyses > 90 % and < 110% concordant were used to generate the age histograms, Concordia diagrams and discuss in the data interpretation (Supplementary Fig. S2). The calculation of the weighted average age and the drawing of Concordia diagrams was done with the Isoplot/Ex (3.0) programme (Ludwig, 2003). Weighted mean ages were calculated at 2s confidence level. The zircon Plešovice was dated as the secondary reference material, yielding a weighted mean ^{206}Pb/^{238}U age of 338.18 ± 5.2 Ma (n = 14, 2 s), which is in excellent agreement with the recommended age of 337.13 ± 0.37 Ma (Sláma *et al.* 2008). The data and zircon U-Pb concordia diagram are at 2 s error. The specific analytical methods and procedures, as well as the common Pb correction, can be found in Andersen (2002, 2005) and Yuan *et al.* (2004).

We intentionally selected detrital zircon grains with different geometric shapes, internal structures, little cracks, and inclusions for testing experiments. A total of 380 zircons are selected for U-Pb dating from the four groups of samples. After discarding the age data with concordance lower 90% and greater 110%, 377 effective concordant age analysis points were obtained (Table S1). For zircons with ages younger than 1000 Ma, ^{206}Pb/^{238}U was used as the best age, while the ages older than 1000 Ma, ^{207}Pb/^{206}Pb was used as the best age. The kernel density estimation (KDE) method was used to visualize all the concordant ages (Vermeesch, 2012).

Uranium-Pb age probability density plots (PDP) of the samples were drawn and analysed visually (e.g. Zhang *et al.* 2020*a*). However, in order to eliminate the influence of subjective judgement on visual analysis and provide a more detailed and quantitative characterization of the similarity among samples, we conducted a quantitative analysis of the similarity of detrital zircon U-Pb age data including cross-correlation coefficient (Saylor *et al.* 2012, 2013), likeness (Satkoski *et al.* 2013), similarity (Gehrels, 2011), a Kolmogorov-Smirnov test (Saylor *et al.* 2012) and multidimensional scaling analysis (MDS) (Vermeesch, 2013; Wissink *et al.* 2018).

4. Results

The zircon crystals in the samples of this study are 75–120 μm in diameter, with subangular–subrounded shapes, and idiomorphic–hypidiomorhic, transparent, prismatic or granular textures, and have length–width ratios of 1.2:1 to 2.5:1 (Supplementary Fig. S2). Most zircon grains show obvious oscillatory growth zoning in CL images. Th/U ratios of zircon can be used to infer a magmatic or metamorphic origin (Wu & Zheng, 2004). All Th/U ratios of samples from the Zusailin Formation with ages younger than 500 Ma are greater than 0.1, while only a few grains older than 500 Ma are less than 0.1 (Fig. 4). The average Th/U ratios of BT-2, BT-3, BT-5 and BT-7 samples are 0.48, 0.53, 0.67 and 0.54, respectively.

https://doi.org/10.1017/S0016756824000116

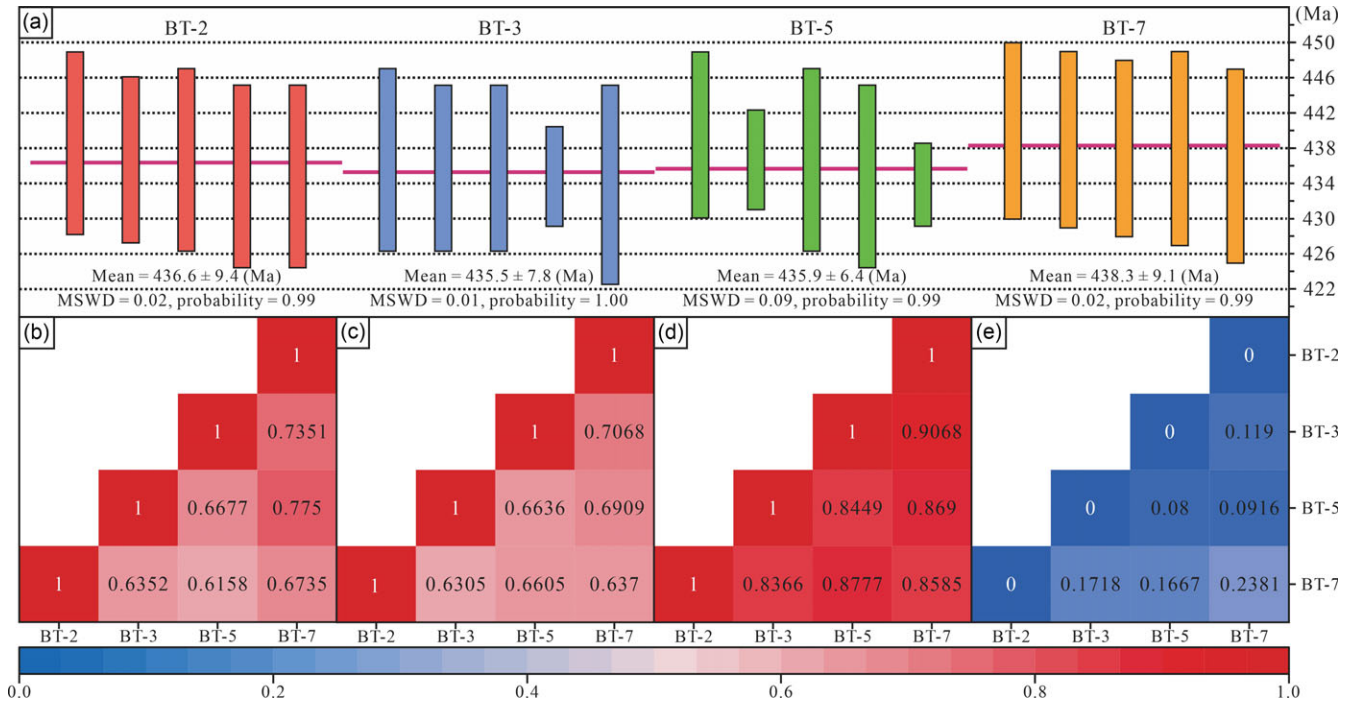

Figure 5. (Colour online) (a) The youngest detrital zircon weighted average age of Zusailing Formation; Similarity analysis among samples; (b) Cross-correlation; (c) Likeness; (d) Similarity; (e) K–S Test D statistic.

Among them, seven zircons in BT-2, three zircons in BT-3, 6 zircons in BT-5 and 3 zircons in BT-7 have Th/U values less than 0.1. Combining the typical oscillatory zoning structure and Th/U ratios of most zircons in the CL images, it can be inferred that most of the detrital zircons from the lower Silurian Zusailing Formation are of magmatic origin, with only a small percentage of metamorphic zircons.

Zircon ages of the Zusailing Formation samples in Nanhao village, Baoting County show distribution from the Mesoarchaean to the early Palaeozoic (434-3174 Ma), with most of them being early Palaeozoic age. The five major peaks are as follows: 2800–2200 Ma, 2100–1350 Ma, 1250–950 Ma, 600–480 Ma and 480–430 Ma and mainly distributed in 480–430 Ma (Supplementary Fig. S1). The major age peak of sample BT-2 is ca. 451 Ma (MSWD = 1.9, $n = 18$), sample BT-3 is ca. 449 Ma (MSWD = 2.4, $n = 12$), sample BT-5 is ca. 448 Ma (MSWD = 3.4, $n = 12$), sample BT-7 is ca.446 Ma (MSWD = 0.62, $n = 13$).

5. Discussion

5.a. Depositional age

In this paper, the age range of the four sample groups is narrow, so the YC2s (weighted mean age corresponding to 2 s) is used to determine the maximum depositional age of the strata (Dickinson & Gehrels, 2009). The YC2s ages of BT-2, BT-3, BT-5 and BT-7 samples are respectively 436.6 ± 9.4 Ma (MSWD = 0.002), 435.5 ± 7.8 Ma (MSWD = 0.01), 435.9 ± 6.1 Ma (MSWD = 0.09) and 438.3 ± 9.1 Ma (MSWD = 0.02) (Fig. 5a). Combined with the abundant palaeontological fossils from the Zusailing Formation, it can be inferred that the maximum depositional age of the Zusailing Formation is Telychian (upper Llandovery).

The results of the similarity analysis of the Zusailing Formation samples (Fig. 5b-e) show that the results of cross-correlation R^2, likeness and similarity are close to 1, while the results of K-S test D statistic are close to 0. Combined with the probability density plot of detrital zircon U-Pb ages (Supplementary Fig. S2), the weighted mean age of the youngest detrital zircon (Fig. 5a), and the chi-square statistics and *p*-values of the Zusailing Formation (Table S4), it can be concluded that the detrital zircon age composition of the Zusailing Formation in the study area is very similar, indicating a common provenance. The four groups of samples from Zusailing Formation are combined and discussed later.

5.b. Sediment sources

The detrital zircon age spectra have 9.2% Archaean ages, 32.9% Palaeoproterozoic ages, 20.5% Mesoproterozoic ages, 13.1% Neoproterozoic ages and 24.3% early Palaeozoic ages. The age peaks are ca. 1769 Ma, ca 1612 Ma, ca. 1430 Ma, ca 1119 Ma, ca. 574 Ma and ca. 449 Ma. The cumulative proportion diagram (Cawood *et al.* 2012) shows that the cumulative curves of the four sample are similar, although a small number of zircons (about 20%) have crystallization ages that are close to the sedimentation age, indicating that the sediment was deposited in a collisional basin (Fig. 6b).

The 2800–2200 Ma and 2100–1350 Ma detrital zircons show euhedral-subhedral morphologies, but they have complex internal structures, characterized by brighter CL images, weak and planar zoning, and metamorphic recrystallization (Supplementary Fig. S1). Therefore, we speculate that the detrital zircons in this age group are likely from nearby areas and/or reflect inputs from multi-cycle sediment sources. Detrital zircons in the Zusailing Formation have main age peaks at ca. 1769 Ma, ca. 1612 Ma and ca. 1430 Ma, as well as multiple small peaks, which are almost identical with the ca. 1.78 Ga, ca. 1.60 Ga and ca. 1.43 Ga age zircons from the Baoban Complex in the basement of Hainan Island (Fig. 7c-f). Previous studies have shown that the complex magmatic

https://doi.org/10.1017/S0016756824000116

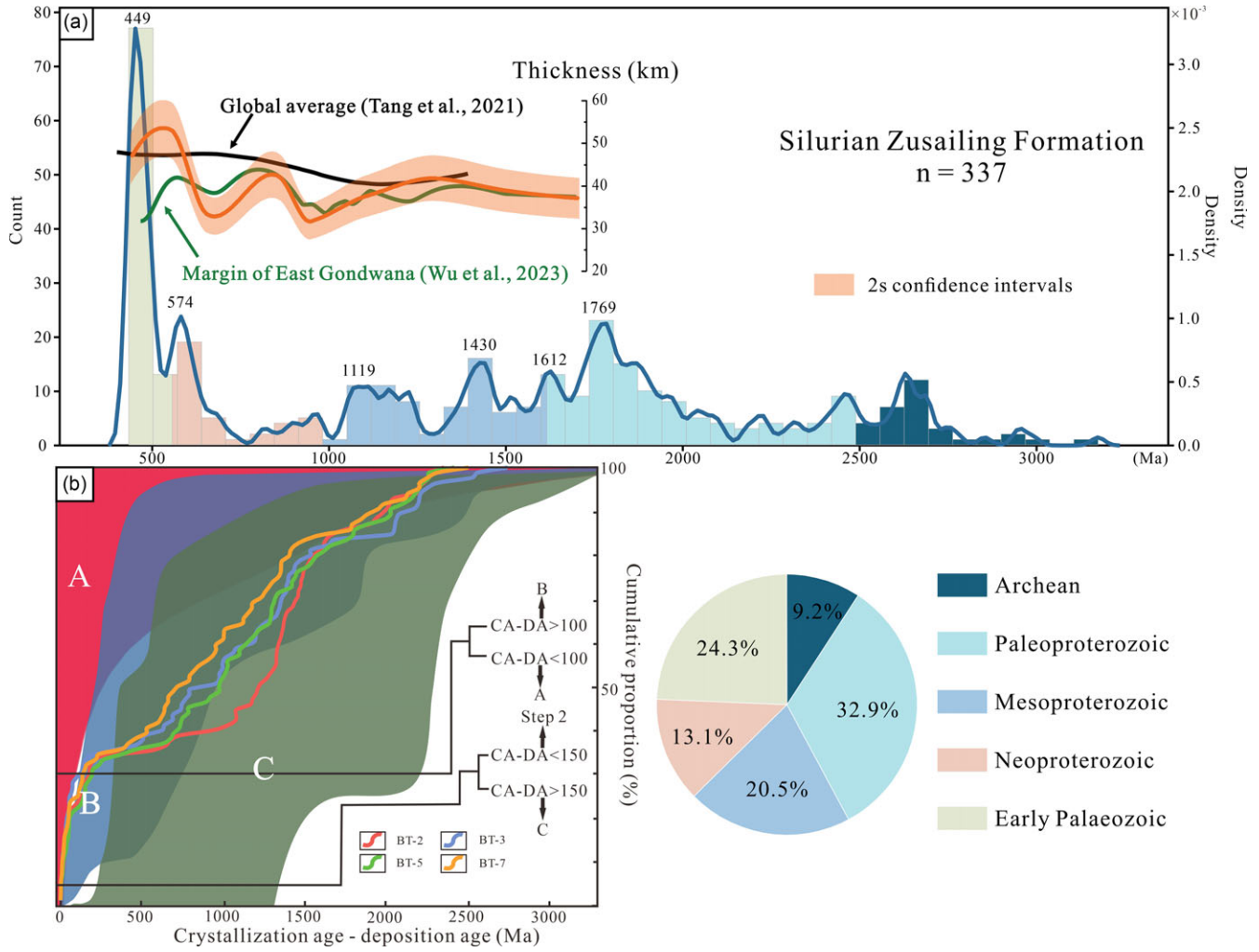

Figure 6. (Colour online) (a) Kernel density estimate (KDE) diagrams of detrital zircon U–Pb ages from Zusailing Formation and Crustal thickness between 435–1800 Ma modelled by zircon anomalies Eu/Eu* (chondrite-normalized Eu/$\sqrt{\text{Sm} \times \text{Gd}}$). The black and green curves represent global compilation (Tang *et al.* 2021) and the margin of East Gondwana continents (after Wu *et al.* 2023); (b) Cumulative ratio curve of the difference between measured crystallization age and sedimentary age of detrital zircons, convergent (A: red field), collisional (B: blue field), extensional settings (C: green field) (after Cawood *et al.* 2012).

and metamorphic events in the Baoban Complex are related to the Nuna (Columbia) supercontinent cycle, and it is highly possible that Hainan Island was connected to western Laurentia and eastern Australia during the Mesoproterozoic to Palaeoproterozoic (Zhou *et al.* 2015*a*; Yao *et al.* 2017; Zhang *et al.* 2018*a*, 2019; Xu *et al.* 2019; Zhao *et al.* 2020, 2021; Suzuki *et al.* 2023). The detrital zircon ages of the Zusailing Formation have similar Mesoproterozoic–Palaeoproterozoic peaks as those of the Belt–Purcell Supergroup in western Laurentia and the lower to middle Rocky Cape Group in Tasmania in eastern Australia. In summary, we argue that the detrital zircon age groups in the samples from 2800–2200 Ma and 2100–1350 Ma record the tectonic events of the Nuna supercontinent, and the ultimate source regions were likely western Laurentia and eastern Australia.

During the Mesoproterozoic–Neoproterozoic Grenvillian Orogeny (1.3–0.9 Ga), the residual fragments of the Columbia supercontinent that were not completely disintegrated converged to form the Rodinia supercontinent (Fig. 7b) (Cawood, 2020; Zhang *et al.* 2020*b*; Wu *et al.* 2023). The Grenvillian Orogeny (1.3–0.9 Ga) is extensively recorded in both Laurentia and Gondwana (Fig. 7c-j). The upper Vindhyan sequence of the Vindhyan Basin in northwestern India contains a large amount of 1200–1000 Ma detrital zircons (McKenzie *et al.* 2013; Turner *et al.* 2014). There is an age peak of 964 Ma and a detrital zircon age group of 1160–1076 Ma in the Cambrian–Devonian sandstone of the Truong Son Belt in the northern Indochina Block (Wang *et al.* 2016, 2021*a*). The Silurian-Ordovician strata in the Perth Basin in Western Australia record 1200–1050 Ma detrital zircons from the Albany-Fraser Belt on the southern margin of the Archaean Yilgarn Craton (Fitzsimons, 2000; Meert, 2003; Wang *et al.* 2016; Olieook *et al.* 2019). In northern East Gondwana, Sibumasu also contains a significant percentage of Greenlandian detrital zircons (Cai *et al.* 2017; Wu *et al.* 2023). But at this time, Sibumasu had not fully formed, with the eastern and western Sibumasu blocks receiving sediment from northern India and western Australia, respectively (Zhang *et al.* 2018*b*). Through the comparison of detrital zircon age groups, we found that both the Vindhyan Basin in northwest India and the Perth Basin in Western Australia contain 1300–900 Ma detrital zircons reflecting the Grenville Orogeny. However, considering the distance between the study area and the Indian Plate when these basins were formed, the possibility of Vindhyan Basin providing detritus to the study area

https://doi.org/10.1017/S0016756824000116

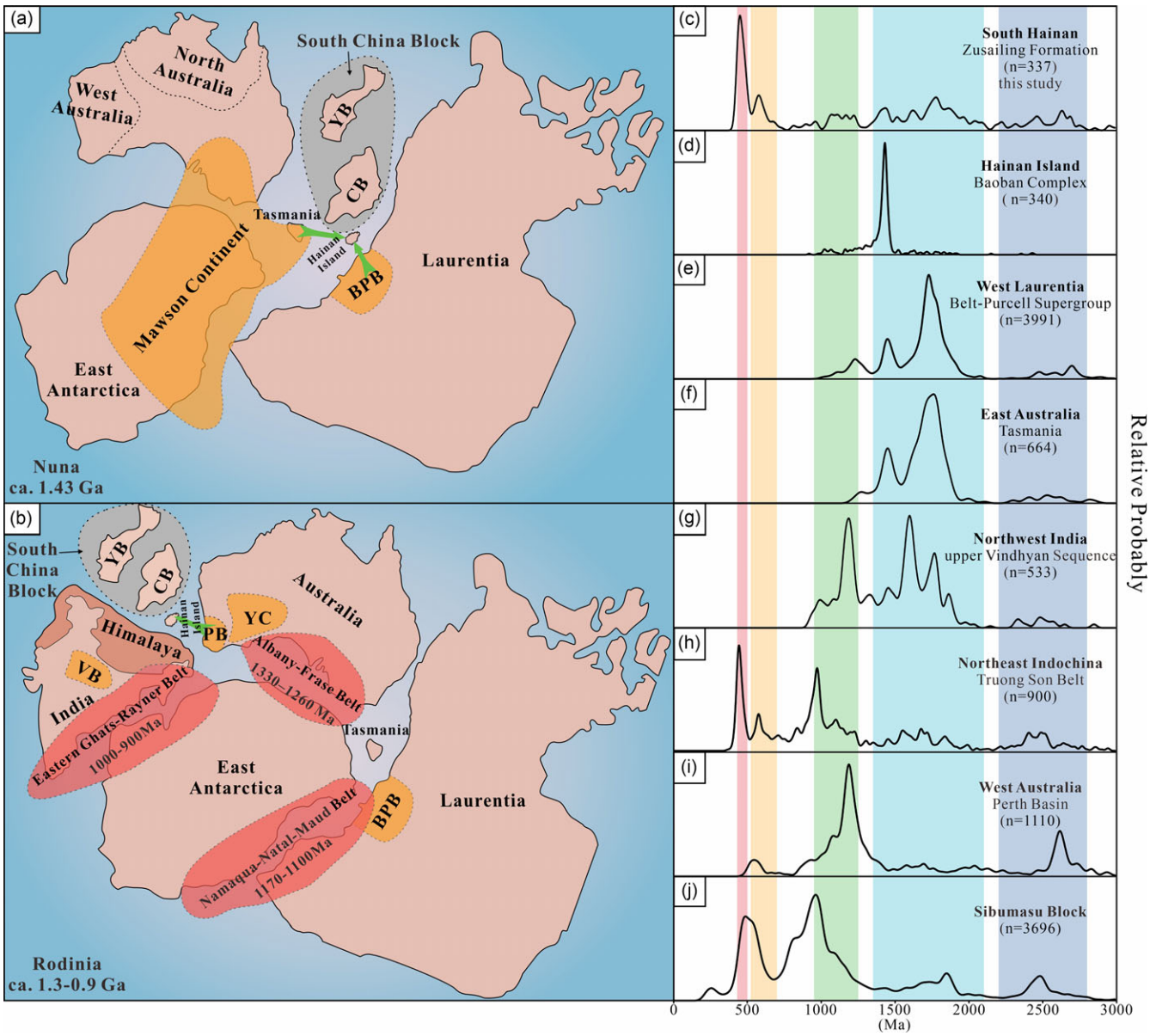

Figure 7. (Colour online) The speculated palaeoposition of Hainan Island and summary of detrital zircon age of distribution of sedimentary rocks of this study and previous work. (a) Showing the connection of Hainan with Laurentia and Australia at –1.43 Ga during the break-up of Nuna (modified after Yao *et al.* 2017; Zhang *et al.* 2018*a*, 2019; Xu *et al.* 2019); (b) showing the proposed configuration of Hainan, Yangtze, Cathaysia, India, Australia, Antarctica and Laurentia at 1.3–0.9 Ga assembly of Rodinia supercontinent (modified after Li *et al.* 2018; Qi *et al.* 2020; Zhang *et al.* 2020*b*; Wu *et al.* 2023); Abbreviations: BPB, Belt-Purcell Basin; CB, Cathaysia Block; PB, Perth Basin; VB, Vindhyan Basin; YB, Yangtze Block; YC, Yilgarn Craton. Green arrows show hypothetical transport pathways of sediments from sources. (c) South Hainan Island; (d) Baoban Complex from Hainan Island ; (e) Belt-Purcell Supergroup from western Laurentia; (f) lower to middle part of the Rocky Cape Group from Tasmania; (g) lower-middle Rocky Cape Group from Tasmania; (h) Truong Son Belt in Central Vietnam and Eastern Laos; (i) Perth Basin in west Australia; (j) Sibumasu. Data sources for (c) – this study; (d) – Li *et al.* 2002, 2008; Yao *et al.* 2017; Zhang *et al.* 2018*a*; (e) – Ross *et al.* 1991, 1992; Rämö *et al.* 2003; Ross & Villeneuve, 2003; Link *et al.* 2007; Stewart *et al.* 2010; Doe *et al.* 2012; Malone *et al.* 2017; Mulder *et al.* 2017; (f) – Black *et al.* 2004; Halpin *et al.* 2014; Mulder *et al.* 2016; (g) – Malone *et al.* 2008; Mckenzie *et al.* 2011, 2013; Turner *et al.* 2014; (h) – Wang *et al.* 2016, 2021*a*; (i) – Cawood & Nemchin, 2000; Veevers *et al.* 2005; Condie *et al.* 2009; (j) – Cai *et al.* 2017; Wu *et al.* 2023. All data are based on analyses within 90–110% of concordance. n=number of concordant analyses.

was excluded. On the other hand, plates such as the Truong Son Belt and Sibumasu formed relatively later, and their Neoproterozoic detrital zircons are of a recycled origin. Therefore, the provenance of the 1250–950 Ma detrital zircons in the sample may be the Albany–Fraser Belt in Western Australia.

During the Pan-African Orogeny (ca. 550 Ma), subduction of the proto-Tethys Ocean caused a series of microcontinents to coalesce to the northern margin of East Gondwana (Wang *et al.* 2016; Zhou, 2018; Qi *et al.* 2020; Zhou *et al.* 2021*a*; Du, 2022; Wu *et al.* 2023). Palaeomagnetic results show that during the Pan-African Orogeny, India, East Antarctica, and Australia converged to form East Gondwana (Fitzsimons, 2000, 2003; Powell et al., 2001; Pisarevsky et al., 2003). From 570 to 510 Ma, the collision of India–Antarctica and Australia–Antarctica resulted in the formation of the Kuunga Orogeny (Meert, 2003; Meert & Lieberman, 2008; Boger, 2011). The area between India and Western Australia, which is called the Pinjarra Orogen (Fitzsimons, 2003; Harley *et al.* 2013), records significant regional deformation and high-grade metamorphism because of convergence (Halpin *et al.* 2008; Pankhurst *et al.* 2008; Boger, 2011).

https://doi.org/10.1017/S0016756824000116

However, there are no magmatic events in South China (Yangtze and Cathaysia Blocks) during this period (Wang *et al.* 2010). In summary, we argue that the ca. 574 Ma age peak and 600–480 Ma detrital zircon in the samples record the tectonic cycles of the Gondwana and the source area was the Pinjarra Orogen between India and Western Australia.

The 480–430 Ma detrital zircons show a significant ca. 449 Ma age peak, and the zircons exhibit typical magmatic zoning with euhedral to subhedral crystals (Supplementary Fig. S2), indicating that most of the sediments were deposited proximally. In the north of Baoting County, rocks of this age are widely reported. A 453–448 Ma andesite rock related to subduction events have been identified in Bangxi and Tunchang areas in northern Hainan Island (Zhou *et al.* 2021*b*; Du, 2022). Under the influence of Kwangsian Orogeny, the Wuyi-Yunkai Orogen in the Cathaysia Block preserves many early Palaeozoic magmatic and metamorphic records, most of which are S-type granites. These granites are mainly derived from Precambrian basement with limited mantle-derived components (Li *et al.* 2010; Liu *et al.* 2010; Xia *et al.* 2014). Provenance studies of lower Palaeozoic strata in South China indicate that the detritus in the Yangtze block originated from the rocks associated with the Kwangsian orogeny in the Cathaysia Block (Xu *et al.* 2012, 2013; Wang *et al.* 2010). The main Silurian strata exposed north of the Jianfeng-Diaoluo fault in the Hainan Island is the Tuolie Formation, which comprises a regressive sedimentary sequence of deep to bathyal to shallow sea origin (Yao *et al.* 1999; Zeng *et al.* 2003). However, the Tuolie Formation is not exposed in the study area on the south side of the Jianfeng-Diaoluo fault. Here, the Silurian strata show regression through a succession of shallow marine, neritic shelf, and foreshore or nearshore origin consisting of S_1k, S_1d, S_1kq and S_2z (Zeng *et al.* 2003, Li *et al.* 2007). In conclusion, the Silurian deposits on Hainan Island suggest regression, evident in both the deeper water sequences to the north and the shallower water sequences to the south. Furthermore, the Zusailing Formation was neither sourced from the ca. 450 Ma rocks in the north of Baoting County nor from the ca. 440-Ma-old detritus widespread in early Palaeozoic sedimentary rocks in South China. We propose that the ca. 449 Ma age peak in the detrital zircon ages of the Zusailing Formation likely signifies a hitherto unidentified tectonic event in southern Hainan Island. The provenance of the Zusailing Formation provides sedimentary evidence for a more detailed and accurate reconstruction of the early Palaeozoic tectonic evolution of Hainan Island and its position within East Gondwana.

5.c. Early Silurian tectonic environment in the Hainan Island

Trace elements indicate that the magmatic zircons are mostly derived from granitoids (Fig. 8a-d). Relative to the primitive mantle, U is usually significantly enriched and Yb is slightly depleted in island arc magma, resulting in a higher U/Yb ratio than mid-ocean-ridge basalt (MORB) (Grimes *et al.* 2015). In the diagram of U/Yb-Hf and U/Yb-Y zircon genesis, most of the 600–434 Ma detrital zircons in the Zusailing Formation, indicate that the zircons are predominantly of continental crust origin (Fig. 8e, f). The relative contents of Th, U, Hf and Nb in zircon can reflect the tectonic background during crystallization, and the differences in these elements can be used to distinguish the tectonic background of host magmas. Niobium depletion of arc magma is more obvious than that of intraplate magma, so the zircons formed by arc magma crystallization have lower Nb/Hf ratio and higher Th/Nb ratio (Yang *et al.* 2012*a*, *b*). In the Nb/Hf-Th/U and Hf/Th-Th/Nb diagrams, the 434–600 Ma detrital zircons from the Zusailing Formation samples almost all plot in the island arc/orogenic belt field (Fig. 8g, h). Considering that the detrital zircons are mainly formed in the continental crust, it can be inferred that the 434–600Ma detrital zircons in the Zusailing Formation samples record orogenic events on the southern side of Hainan Island.

Recently, the application of Eu anomaly (Eu/Eu*) of detrital zircon as a chemical mohometer to estimate crustal thickness has gained widespread use (Tang *et al.* 2020, 2021; Brudner *et al.* 2022; Carrapa *et al.* 2022; Gao *et al.* 2022a; Wu *et al.* 2023). In this paper, we used zircon europium anomaly [chondrite-normalized (Sun & McDonough, 1989) $Eu/\sqrt{(Sm\times Gd)}$] based empirical equation of detrital zircons from Zusailing Formation to estimate the crustal thickness during Mesoproterozoic to Early Palaeozoic in the provenance region (Fig. 6a). The empirical equation calculates crustal thickness (Tang *et al.* 2020):

$$z = (84.2 \pm 9.2) \times Eu/Eu * zircon + (24.5 \pm 3.3)$$

where z is the crustal thickness (in km). To eliminate the influence of metamorphic zircons and those affected by inclusions, data with Th/U<0.1 and/or La>1 parts per million (ppm) are removed before calculating the crustal thickness (Hoskin & Schaltegger, 2003). The highest 10% and the lowest 10% Eu/Eu* data within 5-year intervals are removed when the average crustal thickness is calculated. This selection method will only reduce the scatter of data and will not change the calculated crustal thickness pattern. Our estimate of the crustal thickness of the Hainan Island region before ca. 600 Ma is in good agreement with the continental thickness of the margin of East Gondwana (Wu *et al.* 2023). However, after ca. 600 Ma, the crustal thickness of the Hainan Island region rapidly increased and even exceeded the average thickness of crust, based on global compilations (Tang *et al.* 2021). Thick continental crust usually occurs in continental arcs (Ducea *et al.* 2015; Tang *et al.* 2020), and in Bangxi and Tunchang areas in the northern Hainan Island, there are 453Ma-448Ma andesites that are associated with subduction (Zhou *et al.* 2021b; Du, 2022). Thickened crust reflects the uplift of the sediment source area, which is consistent with the transformation of the lower Silurian strata, recording a transition from marine to terrestrial in Hainan Island. Therefore, the sedimentary environment of the Zusailing Formation in the Hainan Island is back-arc basin in a continental arc, recording the event of crustal thickening between 600 to 434 Ma on the southern side of Hainan Island.

5.d. Sedimentary response to the closure of the Proto-Tethys Ocean

The age spectrum of detrital zircons from the lower Silurian Zusailing Formation in the Hainan Island is compared with those of the Silurian–Devonian strata in northern East Gondwana, including Truong Son, Kontum, Baoshan, Sibumasu, Western Australia, Lhasa, South and North Qiangtang, as well as the Cathaysia and Yangtze Blocks (Fig. 9a-l). We found that the Simao Block, the Truong Son Block of the northern Indochina Block, Kontum of the southern Indochina Block, Baoshan, Sibumasu, Western Australia, Lhasa, and southern Qiangtang have similar ca. 574 Ma age peaks and 600–480 Ma age groups to the samples in this study, indicating that these microcontinents might have recorded Pan-African tectonic events, received sediment from the Kuunga Orogeny and were relatively close to the orogenic belt (Fig. 10a). The majority of the ca. 600–434 Ma detrital zircons from

https://doi.org/10.1017/S0016756824000116

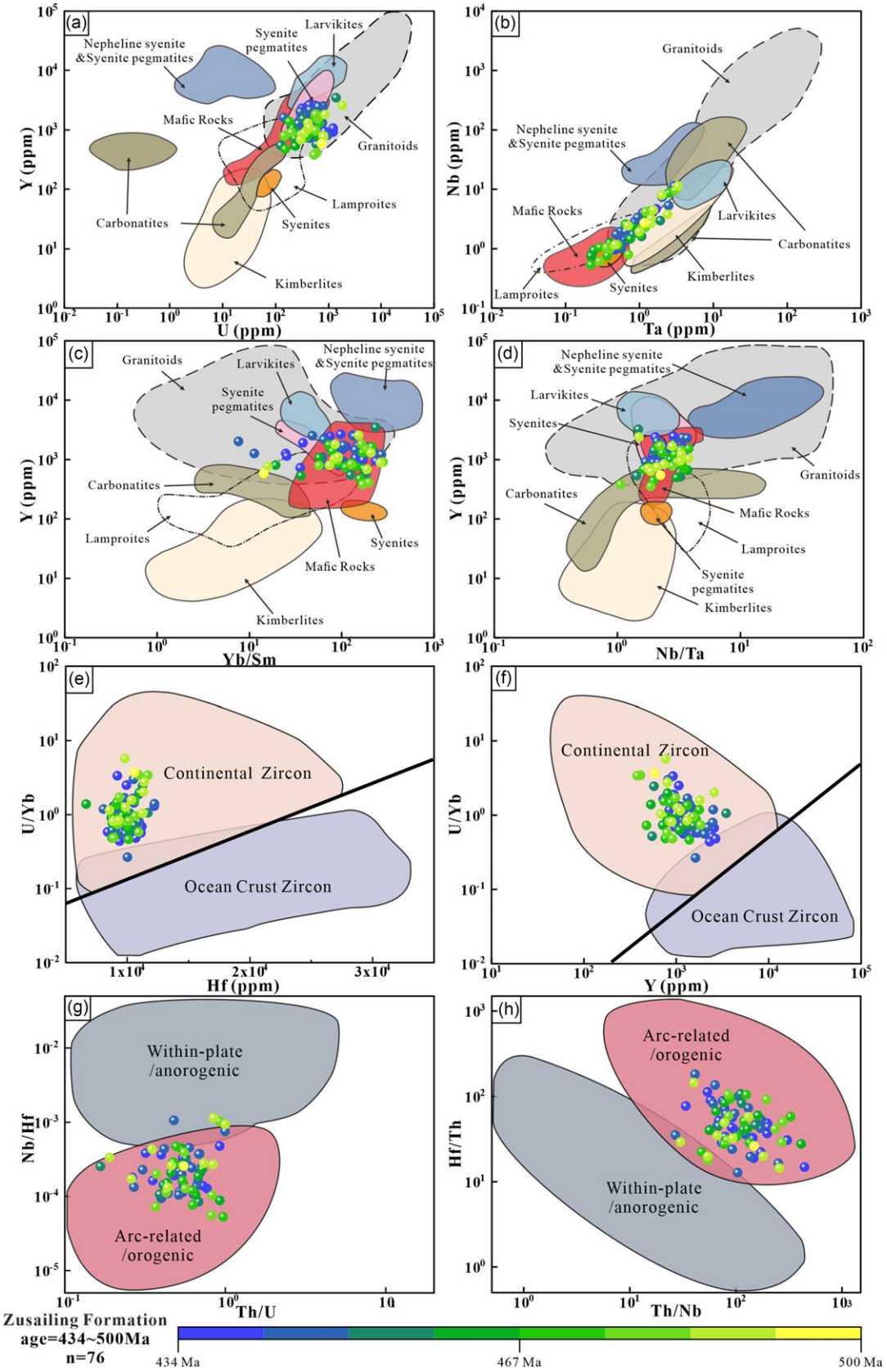

Figure 8. (Colour online) Trace element diagrams of Palaeozoic zircon grains from dated samples in the Zusailing Formation. (a) Y–U; (b) Nb–Ta; (c) Y–Tb/Sm; (d) Y–Nb/Ta (after Belousova *et al.* 2002); (e) U/Yb–Hf; (f) U/Yb–Y (after Grimes *et al.* 2007); (e) Nb/Hf–Th/U; (f) Hf/Th–Th/Nb (after Yang *et al.* 2012*a*, *b*).

https://doi.org/10.1017/S0016756824000116

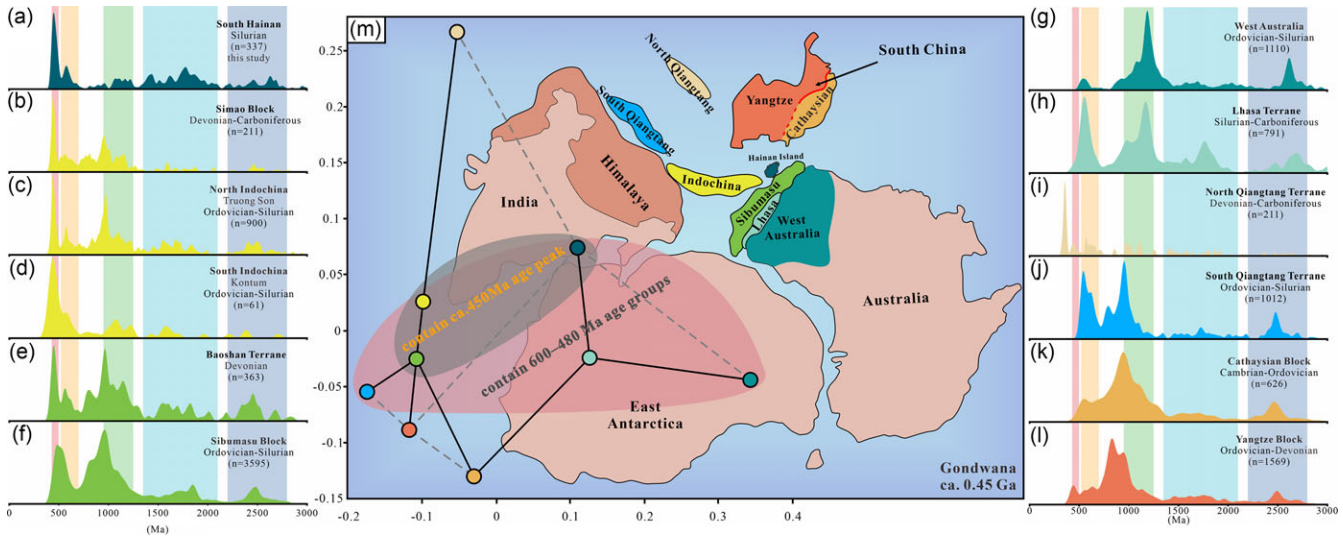

Figure 9. (Colour online) Comparison of the provenance of each microcontinent along the northern margin of East Gondwana. (a) Hainan Island; (b) Simao Block; (c) North Indochina Truong Son; (d) South Indochina Kontum;(e) Baoshan Terrane; (f) Sibumasu Block; (g) West Australia; (h) Lhasa Terrane; (i) North Qiangtang Terrane; (j) South Qiangtang Terrane; (k) Cathaysian Block; (l) Yangtze Block. Data sources for (a) – this study; (b) – Xia *et al.* 2016; Zhao *et al.* 2017; (c) – Wang *et al.* 2016, 2021*a*; (d) – Wang *et al.* 2021*a*; (e) – Nie, 2016; (f) – Cai *et al.* 2017; Wu *et al.* 2023;(g) – Cawood & Nemchin, 2000; Veevers *et al.* 2005; Condie *et al.* 2009; (h) – Leier *et al.* 2007; Zhu *et al.* 2011; Wang *et al.* 2021*c*; (i) – Peng *et al.* 2019; Fu *et al.* 2022; (j) – Pullen *et al.* 2008; Dong *et al.* 2011; Zhu *et al.* 2011; Liu *et al.* 2022*b*; (k) – Wang *et al.* 2010; Yao *et al.* 2011; (l) – Wang *et al.* 2010; Duan *et al.* 2011; Xu *et al.* 2012; Yang *et al.* 2012*a*, *b*; Xia *et al.* 2016; Ma *et al.* 2018; Ren *et al.* 2023. All data are based on analyses within 90–110% of concordance. n=number of concordant analyses. (m) Showing the proposed configuration of Northeastern Gondwana at ca. 0.45 Ga during assembly of the Gondwana supercontinent. (The MDS plot is based on the Kolmogorov-Smirnov (K-S) statistical approach, which is used to separate zircon grains that came from various sources. Different coloured dots correspond to the colours of the microcontinents and KDE diagrams of detrital zircons from them. There is no weight significance for the X and Y axes and do not reflect the real numerical difference. The samples with the highest similarity values are plotted closest to each other. Solid and dashed lines connect the samples with their closest and second-closest neighbours in this plot, respectively.) (modified after Xu *et al.* 2014; Zhang *et al.* 2018*b*; Qi *et al.* 2020; Zhou *et al.* 2021*a*; Zhang *et al.* 2022, 2023; Dodd *et al.* 2023; Wu *et al.* 2023).

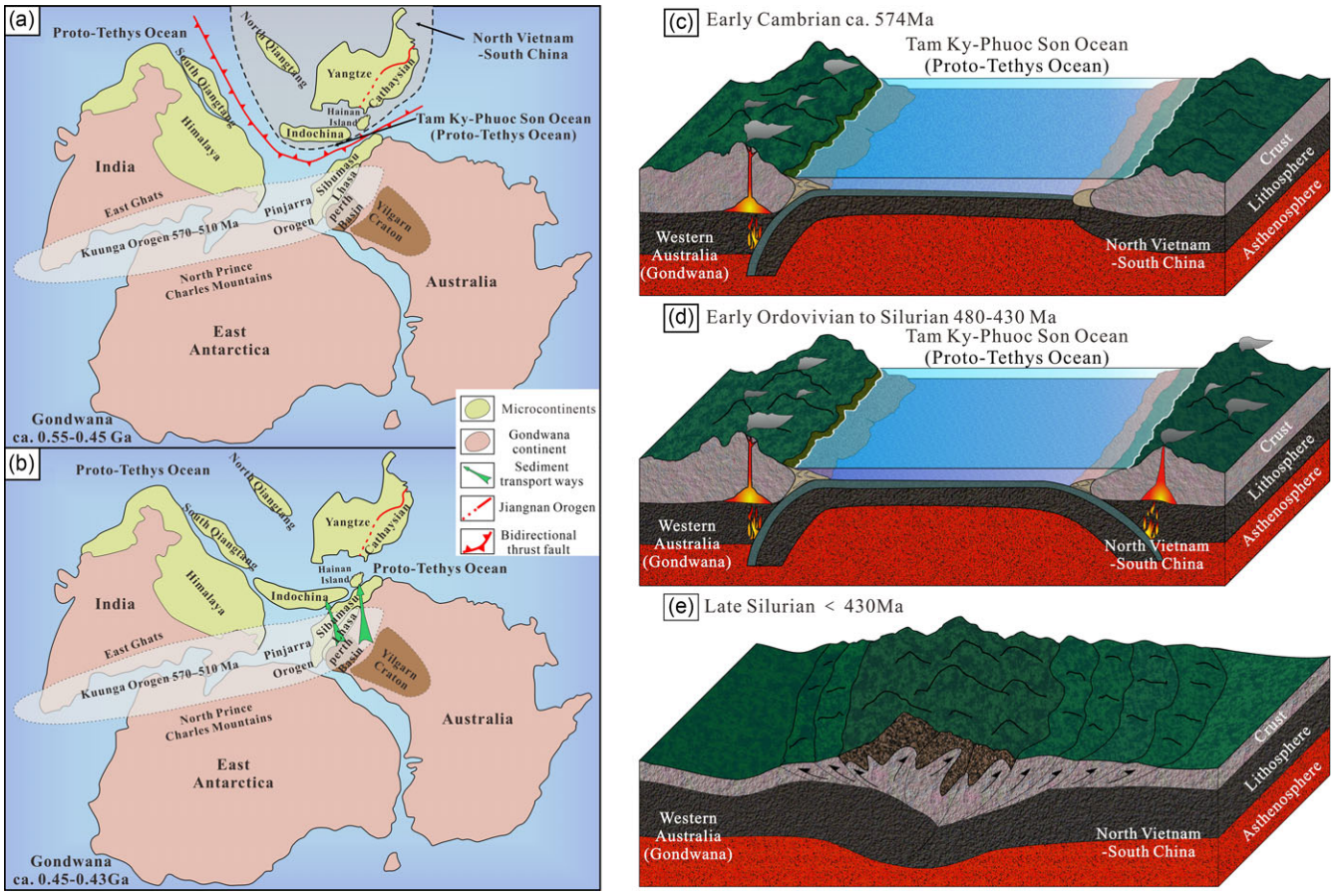

Figure 10. (Colour online) Reconstruction of the Palaeogeography and Tectonic Evolution of the Eastern Proto-Tethys Ocean during Neoproterozoic-Palaeozoic. (modified after Xu *et al.* 2014; Zhang *et al.* 2018*b*; Qi *et al.* 2020; Zhou *et al.* 2021*a*; Zhang *et al.* 2022, 2023; Dodd *et al.* 2023; Wu *et al.* 2023).

https://doi.org/10.1017/S0016756824000116

the lower Silurian Zusailing Formation in the Hainan Island were crystallized in granitic melts in continental crust. The tectonic setting of the granites is island arc/orogenic belt, recording the subduction of the Proto-Tethys Ocean during Neoproterozoic to early Palaeozoic. However, the evolution of the Proto-Tethys Ocean along the northern margin of the entire Gondwana is different. A large number of rock formations related to the subduction of the Proto-Tethys Ocean have been found along the northern margin of the West Gondwana, such as 576–536 Ma granitic rocks and 579–536 Ma metabasic rocks in Kuh-e-Sarhangi area, central Iran (Rossetti *et al.* 2015; Hosseini *et al.* 2015), 512–467 Ma granitic rocks and included ca. 477 Ma crustal xenoliths from central-western Nepal (Cawood *et al.* 2007), Andean-type granites of 480-466 Ma in the Utla and Mansehra regions of northwestern Pakistan (Sajid *et al.* 2018). There is also a lot of evidence for the subduction of the Proto-Tethys Ocean in the northern margin of India-Australia in East Gondwana. The Lhasa Terrane reported 522–496 Ma ultrapotassic rhyolites, 536–492 Ma meta-rhyolite, and 492 Ma meta-basalt (Zhu *et al.* 2012; Ding *et al.* 2015). The 505–468 Ma granitic gneisses and a small amount of 463±5 Ma meta-basalts in the South Qiangtang Terrane (Guynn *et al.* 2012; Peng *et al.* 2014), 502–471Ma magmatism in Gemuri area (Wang *et al.* 2020) and the Duguer region has also reported Late Silurian high-pressure eclogites (Zhang *et al.* 2014). The Tengchong Terrane has widely distributed 488–484 Ma leucogranites, 495–487 Ma granite gneisses and 492-485 Ma light-coloured granites (Eroğlu *et al.* 2013; Wang *et al.* 2013*a*; Zhao *et al.* 2016). The Proto-Tethys Ocean subducted towards the northern margin of the Gondwana, with the western part earlier than the eastern part, and initiation of the subduction towards the northern margin of the India-Australia in East Gondwana should not be later than the Early Cambrian (Fig. 10). The ca. 574 Ma peak age in the lower Silurian Zusailing Formation of the Hainan Island and the detrital zircons of the 600–480 Ma age group reflect this subduction event. The provenance of Hainan Island at this time should be the Pinjarra Orogen between India and Western Australia.

The Simao Block, Truong Son in the northern Indochina Block, Kontum in southern Indochina Block, Baoshan Terrane and Sibumasu Block all have 480–430 Ma detrital zircon age groups. Multidimensional scaling analysis (MDS) is often used for statistical comparison of detrital zircon age compositions and potential provenance or adjacent topography (Vermeesch, 2013). The MDS plot based on the Kolmogorov-Smirnov (K-S) statistical method (Fig. 9m), shows that the Silurian Zusailing Formation in the Hainan Island has a strong affinity with the Simao Block, Truong Son in the northern Indochina Block, Kontum in southern Indochina Block, Baoshan Terrane and Sibumasu Block. This indicates that during 480-430 Ma, these microcontinents were in close proximity to each other in the region, and may be in the same source-to-sink system, recording similar tectonic events (Fig. 10). The South China Block shows a younger age peak of ca. 420 Ma, and does not have the ca. 574 Ma age peak discussed above, which is significantly different from other microcontinents (Fig. 9k, l). Our interpretation is that during formation of East Gondwana in the early Palaeozoic, the far-field response of subduction and collision of the Proto-Tethys Ocean towards the South China Block triggered the intracontinental orogeny (Kwangsian intracratonic orogenic), forming Wuyi-Yunkai Orogen (Wang *et al.* 2010; Xu *et al.* 2012, 2013; Du, 2022). This indicates that the South China Block was further away from the main subduction zone of the Proto-Tethys Ocean and other microcontinents (Fig. 10a, b), which resulted in it being affected by the Proto-Tethys Ocean subduction later than the microcontinents. The amphibolite facies metamorphism of 462 Ma in the Hainan Island is similar to the granulite age of 468 Ma in the Indochina (Faure *et al.* 2018; Zhang *et al.* 2022). In addition, the $\varepsilon_{Hf}(t)$ values of detrital zircons from the Ordovician–Silurian (460–430 Ma) in the Hainan Island and Indochina are also very similar (Zhang *et al.* 2023). These phenomena are all related to the collision closure of the Proto-Tethys branch ocean (Tran *et al.* 2014; Wang *et al.* 2021*a*, *b*; Nguyen *et al.* 2019). Hainan Island was closer to Indochina block in the early Palaeozoic. The ocean basin between Hainan Island and East Gondwana in the early Palaeozoic was an extension of the Tam Ky-Phuoc Son Ocean, which was a larger branch ocean basin of the Proto-Tethys Ocean adjacent to the northern margin of India-Australia.

This study shows that there was a transition from a marine to a continental environment in the Hainan Island region during the early Silurian. The 480–430 Ma detrital zircons in the Zusailing Formation were supplied by the granites of a continental arc. The crustal thickness estimated by the Eu anomaly of the detrital zircons reflects the subduction of the Proto-Tethys Ocean in southern Hainan Island at that time, which thickened the crust under the Andean-type orogenic zone. Meanwhile, the subduction of the Proto-Tethys Ocean underneath northern East Gondwana during the Ordovician to Silurian is also widely recorded. In southwestern Yunnan, there are ophiolitic melanges in the Longmucuo-Shuanghu and the Changning-Menglian suture zones (Liu *et al.* 2017, 2021), abundant high-pressure metamorphic rocks in the Lancang Group (Peng *et al.* 2022), 459–456 Ma Huimin metamorphic volcanic rocks (Nie, 2016; Xing, 2016), 445–439Ma Nantinghe gabbro (Wang *et al.* 2013*b*; Nie, 2016). The Truong Son, Tam Ky-Phuoc Son and Kontum areas in the Indochina block have abundant evidence of magmatic activities related to the bidirectional subduction of the Early Palaeozoic Tam Ky-Phuoc Son Ocean (Shi *et al.* 2015; Nakano *et al.* 2021; Wang *et al.* 2021*a*, *b*). The Sukhothai Terrane belonged to the Indochina Block in the Early Palaeozoic, and the 450-420 Ma feldspar/quartz schist in this area was formed in the plate collision environment (Nie, 2016). The Simao Block is considered to be the extension of the Indochina Block, and there is a great abundance of 446–420 Ma magmatic rocks related to the subduction of the Proto-Tethys Ocean in this area (Liu *et al.* 2018, 2019; Zhao, 2019). The Baoshan Block, which is generally recognized as the northward extension of the Sibumasu, has 499 ± 2 Ma meta-basalt and 502-448 Ma granite rocks related to the retreat or break-off of the Proto-Tethys Oceanic (Yang *et al.* 2012*c*; Dong *et al.* 2013; Metcalfe, 2013; Wang *et al.* 2013*b*; Li *et al.* 2016; Zhang *et al.* 2018*a*; Zhou *et al.* 2020). However, Sibumasu did not separate from Western Australia in the Early Palaeozoic and thus records the characteristics of Gondwana (India-Australia) (Metcalfe, 2013; Liu, 2020; Gao *et al.* 2023), whereas the Hainan Island and the Indochina block have the characteristics of North Vietnam-South China (Xing, 2016; Zhao, 2019; Dan *et al.* 2022). The subduction of the Proto-Tethys Ocean along the northern margin of the East Gondwana in the late Palaeozoic was bidirectional. In the late Neoproterozoic to early Cambrian, the Proto-Tethys Ocean only subducted towards the northern edges of India and Australia. By the end of the early Palaeozoic, the Proto-Tethys Ocean kept subducting towards the northern edges of India-Australia while increasing its subduction to the North Vietnam-South China (from unidirectional to bidirectional subduction) (Fig. 10c, d). The ca. 449 Ma age peak of the Early Siluria Zusailing Formation and the 480–430 Ma detrital

https://doi.org/10.1017/S0016756824000116

zircons age group in the Hainan Island well record the subduction events of the Proto-Tethys Ocean, with the provenance of the continental arc formed by the southward subduction of the Proto-Tethys Ocean towards Hainan Island (Fig. 10b, d). Additionally, due to the bidirectional subduction of the Proto-Tethys Ocean, Hainan Island collided with the Sibumasu on the margin of Western Australia in the early Silurian, resulting in a transformation of the sedimentary environment of Hainan Island from marine to continental and an influx of material from the Pinjarra Orogen. After the collision, the southern part of Hainan Island uplifted and remained in a state of weathering and erosion for a long time (Fig. 10e). In the late Palaeozoic, the break-up of the Gondwana caused Hainan Island to separate from Western Australia, so that the magmatic rocks with subduction-collision related information were eroded or collapsed in the basin, with the result that no early Palaeozoic subduction-collision magmatic rocks were discovered in the southern part of Hainan Island.

In summary, the age spectrum of detrital zircons from the Zusailing Formation in the Hainan Island shows peaks at ca. 574 Ma and ca. 449 Ma, which reflect two tectonic events. The ca. 574 Ma age peak records the subduction of the Proto-Tethys Ocean beneath the northern margin of India-Australia in East Gondwana, and the ca. 449 Ma age peak records the subduction of the Proto-Tethys Ocean beneath the North Vietnam-South China. The microcontinents in northern East Gondwana documenting the closure of the Proto-Tethys Ocean can be roughly divided into two stages. The first stage, 600–480 Ma, records subduction of the Proto-Tethys Ocean towards the northern margins of India-Australia, and the subduction began no later than the Early Cambrian. In the second stage, 480–430 Ma (youngest records in the South China Block), there was subduction of the Proto-Tethys Ocean towards the North Vietnam-South China.

6. Conclusion

(1) The detrital zircon U-Pb ages of the Zusailing Formation in the early Silurian exhibit five age groups of 2800–2200 Ma, 2100–1350 Ma, 1250–950 Ma, 600–480 Ma and 480–430 Ma and are mainly distributed in 500–430 Ma, with a ca. 449 Ma age peak. The 2800–2200 Ma and 2100–1350 Ma detrital zircons are derived from the ancient basement of Hainan Island, with inferred provenance from western Laurentian craton and eastern Australia. The 1250-950Ma detrital zircons are sourced from the Albany-Fraser belt in Western Australia. The provenance of the 600–480Ma detrital zircons is the Pinjarra Orogen located between India and Western Australia. The 480–430 Ma detrital zircon source area is a continental arc formed by the subduction of the Proto-Tethys Ocean to the south of Hainan Island.

(2) The subduction of the Proto-Tethys Ocean beneath the northern margin of India–Australia in East Gondwana had been unidirectional from 600 to 480 Ma. Moreover, from 480 to 430 Ma, the Proto-Tethys Ocean evolved to subduct beneath both East Gondwana and North Vietnam-South China, which includes Hainan Island (bidirectional subduction). The two age peaks of ca. 574 Ma and ca. 449 Ma of the Zusailing Formation in the Hainan Island record the tectonic evolution from unidirectional to bidirectional subduction during the closure of the Proto-Tethys Ocean.

Supplementary material. To view supplementary material for this article, please visit https://doi.org/10.1017/S0016756824000116

Availability of data and materials. The datasets collected during the field surveys and analysed during the current study are available from the corresponding author on reasonable request.

Author contributions. GSY, XZJ, KJT, TH, SYM, FHX, MY conceived, designed and carried out the research. XZJ supplied geochemical dates and contributed to the interpretations and discussions of the research. GSY finished the data compilation, manuscript and figures. All authors contributed to data interpretation, discussion and revision of the manuscript.

Financial support. This work was supported by the National Natural Science Foundation of China (Grant number: 41872101).

Competing interests. The authors declare that there is no conflict of interest regarding the publication of this article.

Reference

Andersen T (2002) Correction of common lead in U-Pb analyses that do not report ^{204}Pb. *Chemical Geology* **192**, 59–79. doi: 10.1016/s0009-2541(02)00195-x.

Andersen T (2005) Detrital zircons as tracers of sedimentary provenance: limiting conditions from statistics and numerical simulation. *Chemical Geology* **216**, 249–70. doi: 10.1016/ j. chemgeo.2004.11.013.

Belousova E, Griffin W, O'Reilly SY and Fisher N (2002) Igneous zircon: trace element composition as an indicator of source rock type. *Contributions to Mineralogy and Petrology* **143**, 602–22. doi: 10.1007/s00410-002-0364-7.

Black LP, Calver CR, Seymour DB and Reed A (2004) SHRIMP U-Pb detrital zircon ages from Proterozoic and Early Palaeozoic sandstones and their bearing on the early geological evolution of Tasmania. *Australian Journal of Earth Sciences* **51**, 885–900. doi: 10.1111/j.1400-0952.2004.01091. x.

Boger SD (2011) Antarctica—Before and after Gondwana. *Gondwana Research* **19**, 335–71. doi: 10.1016/j.gr.2010.09.003.

Brudner A, Jiang H, Chu X and Tang M (2022) Crustal thickness of the Grenville orogen: a Mesoproterozoic Tibet? *Geology* **50**, 402–6. doi: 10.1130/G49591.1.

Burrett C, Zaw K, Meffre S, Lai CK, Khositanont S, Chaodumrong P, Udchachon M, Ekins S and Halpin J (2014) The configuration of Greater Gondwana—Evidence from LA ICPMS, U–Pb geochronology of detrital zircons from the Palaeozoic and Mesozoic of Southeast Asia and China. *Gondwana Research* **26**, 31–51. doi: 10.1016/j.gr.2013.05.020.

Cai FL, Ding L, Yao W, Laskowski AK, Xu Q, Zhang JE and Sein K (2017) Provenance and tectonic evolution of lower Paleozoic–upper Mesozoic strata from Sibumasu terrane, Myanmar. *Gondwana Research* **41**, 325–36. doi: 10.1016/j.gr.2015.03.005.

Cai ZH, Xu ZQ, Duan XD, Li HQ, Cao H and Huang XM (2013) Early stage of Early Paleozoic orogenic event in western Yunnan Province, southeastern margin of Tibet Plateau. *Acta Petrologica Sinica* **29**, 2123–40. doi: 10.2113/gssajg.116.1.169.

Carrapa B, DeCelles PG, Ducea MN, Jepson G, Osakwe A, Balgord E, Goddard ALS and Giambiagi LA (2022) Estimates of paleo-crustal thickness at Cerro Aconcagua (Southern Central Andes) from detrital proxy-records: implicationsfor models of continental arc evolution. *Earth and Planetary Science Letters* **585**, 117526. doi: 10.1016/ j. epsl.2022.117526.

Cawood PA (2020) Earth matters: a tempo to our planet's evolution. *Geology* **48**, 525–26. doi: 10.1130/focus052020.1.

Cawood PA, Hawkesworth CJ and Dhuime B (2012) Detrital zircon record and tectonic setting, *Geology* **40**, 875–78. doi: 10.1130/G32945.1.

Cawood PA, Johnson MRW and Nemchin AA (2007) Early Palaeozoic orogenesis along the Indian margin of Gondwana: tectonic response to Gondwana assembly. *Earth and Planetary Science Letters* **255**, 70–84. doi: 10.1016/j.epsl.2006.12.006.

Cawood PA and Nemchin AA (2000) Provenance record of a rift basin: U/Pb ages of detrital zircons from the Perth Basin, Western Australia. *Sedimentary Geology* **134**, 209–34. doi: 10.1016/S0037-0738(00)00044-0.

Chao HX, Han XH, Yang ZH, Wu X, Lv Y, Yang H, Yang LH and Wang LP (2016) New exploration of geotectonic characteristics of Hainan Island. *Earth Science Frontiers* **23**, 200–11. doi: 10.13745/ j.esf.2016.04.017.

Charvet J (2013) The Neoproterozoic–Early Paleozoic tectonic evolution of the South China Block: an overview. *Journal of Asian Earth Sciences* **74**, 198–209. doi: 10.1016/ j. jseaes.2013.02.015.

Chen Q, Sun M, Long XP, Zhao GC and Yuan C (2016) U-Pb ages and Hf isotopic record of zircons from the late Neoproterozoic and Silurian-Devonian sedimentary rocks of the western Yangtze Block: implications for its tectonic evolution and continental affinity. *Gondwana Researc* **31**, 184–99. doi: 10.1016/j.gr.2015.01.009.

Chen ZP, Li SX, Yun P, Lin YH, Wang YH, Chen FY and Gong D (2012) Geological characteristics and age of Nanhao Formation in Nanhao Area, Hainan Province. *Geology in China* **39**, 651–60. doi: 10.1007/s11783-011-0280-z.

Cocks LRM and Torsvik TH (2013) The dynamic evolution of the Palaeozoic geography of eastern Asia. *Earth-Science Reviews* **117**, 40–79. doi: 10.1016/J.EARSCIREV.2012.12.001.

Condie KC, Belousova E, Griffin W and Sircombe KN (2009) Granitoid events in space and time: constraints from igneous and detrital zircon age spectra. *Gondwana Research* **15**, 228–42. doi: 10.1016/j.gr.2008.06.001.

Dan W, Murphy JB, Wang Q, Zhang XZ and Tang GJ (2022) Tectonic evolution of the Proto-Qiangtang Ocean and its relationship with the Palaeo-Tethys and Rheic oceans. *The Geological Society of London* **531**, 249–264. doi: 10.1144/SP531-2022-14.

Deng J, Wang QF and Li GJ (2016) Superimposed orogeny and composite metallogenic system: case study from the Sanjiang Tethyan belt, SW China. *Acta Petrologica Sinica* **32**, 2225–47. doi: CNKI: SUN: YSXB.0.2016-08-001.

Deng J, Wang QF, Li GJ and Zhou DQ (2019) The theory of composite metallogenic system: key of recovering metallogenic mystery in the SW Tethys. *Acta Petrologica Sinica* **35**, 1303–23. doi: 10.18654/1000-0569/2019.05.01.

Dickinson WR and Gehrels GE (2009) U-Pb ages of detrital zircons in Jurassic eolian and associated sandstones of the Colorado Plateau: evidence for transcontinental dispersal and intraregional recycling of sediment. *Geological Society of America Bulletin* **121**, 408–33. doi: 10.1130/B26406.1.

Ding HX, Zhang ZM, Dong X, Yan R, Lin YH and Jiang HY (2015) Cambrian ultrapotassic rhyolites from the Lhasa terrane, South Tibet: evidence for Andean-type magmatism along the northern active margin of Gondwana. *Gondwana Research* **27**, 1616–29. doi: 10.1016/j.gr.2014.02.003.

Dodd MS, Shi W, Li C, Zhang Z, Cheng M, Gu HD, Hardisty DS, Loyd SJ, Wallace MW, Hood AS, Lamothe K, Mills BJW, Poilton SW and Lyons TW (2023) Uncovering the Ediacaran phosphorus cycle. *Nature* **31**, 1–7. doi: 10.1038/s41586-023-06077-6.

Doe MF, Jones JV, Karlstrom KE, Thrane K, Frei D, Gehrels G and Pecha M (2012) Basin formation near the end of the 1.60–1.45 Ga tectonic gap in southern Laurentia. Mesoproterozoic Hess Canyon group of Arizona and implications for ca. 1.5 Ga supercontinent configurations. *Lithosphere* **4**, 77–88. doi: 10.1130/L160.1.

Dong C, Li C, Wan Y, Wang W, Wu Y, Xie H and Liu D (2011) Detrital zircon age model of Ordovician Wenquan quartzite south of Lungmuco-Shuanghu suture in the Qiangtang area, Tibet: constraint on tectonic affinity and source regions. *Science China Earth Sciences* **54**, 1034–42. doi: 10.1007/s11430-010-4166-x.

Dong ML, Dong GC, Mo XX, Santosh M, Zhu DC, Yu JC, Nie F and Hu ZC (2013) Geochemistry, zircon U-Pb geochronology and Hf isotopes of granites in the Baoshan Block, western Yunnan: implications for Early Paleozoic evolution along the Gondwana margin. *Lithos* **179**, 36–47. doi: 10.1016/j.lithos.2013.05.011.

Dong X, Zhang ZM and Santosh M (2010) Zircon U-Pb chronology of the Nyingtri group, Southern Lhasa Terrane, Tibetan Plateau: implications for Grenvillian and Pan-African provenance and Mesozoic-Cenozoic metamorphism. *The Journal of Geology* **118**, 677–90. doi: 10.1086/656355.

Dopieralska J, Belka Z, Königshof P, Racki G, Savage N, Lutat P and Sardsud A (2012) Nd isotopic composition of Late Devonian seawater in western Thailand: geotectonic implications for the origin of the Sibumasu terrane. *Gondwana Research* **22**, 1102–9. doi: 10.1016/j.gr.2012.01.009.

Du JY (2022) Geochemical characteristics and geological significance of early Paleozoic volcanic rocks on Hainan Island. Guilin University of Technology. doi: 10.27050/d.cnki.gglgc.2022.000218.

Du YK, Liu HL, Tan XD, Han YL, Wu Y, Wu CH and Zhao MS (2013) Late paleozoic to mesozoic paleomagnetic results from Hainan Island and its tectonic implications for the northern margin of the South China Sea. *Marine Geology & Quaternary Geology* **33**, 93–103. doi: CNKI: SUN: HYDZ.0.2013-06-014

Duan LA, Meng QR, Zhang CL and Liu XM (2011) Tracing the position of the South China Block in Gondwana: U–Pb ages and Hf isotopes of Devonian detrital zircons. *Gondwana Research* **19**, 141–9. doi: 10.1016/j.gr.2010.05.005.

Ducea MN, Saleeby JB and Bergantz G (2015) The architecture, chemistry, and evolution of continental magmatic arcs. *Annual Review of Earth and Planetary Sciences* **43**, 299–331. doi: 10.1146/annurev-earth-060614-105049.

Eroğlu S, Siebel W, Daniík M, Pfänder JA and Chen FK (2013) Multi-system geochronological and isotopic constraints on age and evolution of the Gaoligongshan metamorphic belt and shear zone system in western Yunnan, China. *Journal of Asian Earth Sciences* **73**, 218–39. doi: 10.1016/j.jseaes.2013.03.031.

Faure M, Nguyen VV, Hoai LTT and Lepvrier C (2018) Early Paleozoic or Early-Middle Triassic collision between the South China and Indochina Blocks: the controversy resolved? Structural insights from the Kon Tum massif (Central Vietnam). *Journal of Asian Earth Sciences* **166**, 162–80. doi: 10.1016/j.jseaes.2018.07.015.

Faure M, Shu LS, Wang B, Charvet J, Choulet F and Monie P (2009) Intracontinental subduction: a possible mechanism for the Early Palaeozoic Orogen of SE China. *Terra Nova* **21**, 360–8. doi: 10.1111/j.1365-3121.2009.00888. x.

Fitzsimons ICW (2000) Grenville–age basement provinces in East Antarctica: evidence for three separates collisional orogens. *Geology* **28**, 879–82. doi: 10.1130/0091-7613(2000)28<879: GBPIEA>2.0.CO;2.

Fitzsimons ICW (2003) Proterozoic basement provinces of Southern and Southwestern Australia, and their correlation with Antarctica. *Geological Society London Special Publications* **206**, 93–130. doi: 10.1144/gsl.sp.2003.206.01.07.

Fu XG, Wang J, Wei HY, Feng XL, Zeng SQ, Zeng YH and Nie Y (2022) Detrital zircons of the Devonian-Permian sandstones in the Qiangtang terrane, Tibet: implication for Qiangtang rifting from Gondwana and uplift history of the Central Uplift. *Journal of Asian Earth Sciences* **239**, 1–11. doi: 10.1016/j.jseaes.2022.105392.

Gao B, Chen J, Huang X, Xin H and Zheng Q (2022a) Resolving the tectonic setting of South China in the late Paleozoic? *Geophysical Research Letters* **49**, 1–11. doi: 10.1029/2022GL099809.

Gao W, Shi JR, Meng QK, Shu Q, Zhang KS, Wang CY and Xu GJ (2022b) Discovery and geological significance of the Indosinian granulites in Hainan Island: new evidence from U-Pb dating and trace element composition of zircons. *ACTA Geological Sinica* **96**, 426–44. doi: 10.19762/j.cnki.dizhixuebao.2022115.

Gao Y, Li G, Liu ZH, Liu JL, Wang C, Xu ZY and Wang CB (2023) Lower Paleozoic detrital zircon U-Pb geochronological characteristics of the Baoshan Block in western Yunnan and its constraints on the Proto-Tethys tectonic evolution. *Acta Petrologica Sinica* **39**, 921–37. doi: 10.18654/1000-0569/2023.03.17.

Gehrels G (2011) Detrital zircon U-Pb geochronology: current methods and new opportunities: tectonics of sedimentary basins. In *Tectonics of Sedimentary Basins: Recent Advances*, pp. 45–62. Blackwell Publishing Ltd. doi: 10.1002/9781444347166.ch2.

Grimes CB, John BE, Kelemen PB, Mazdab FK, Wooden JL, Cheadle ML, Hanghøj K and Chwartz JJ (2007) Trace element chemistry of zircons from oceanic crust: a method for distinguishing detrital zircon provenance. *Geology* **35**, 643–46. doi: 10.1130/G23603A.1.

Grimes CB, Wooden JL, Cheadle MJ and John BE (2015) "Fingerprinting" tectonomagmatic provenance using trace elements in igneous zircon. *Contributions to Mineralogy and Petrology* **170**, 46. doi: 10.1007/s00410-015-1199-3.

Guynn J, Kapp P, Gehrels GE and Ding L (2012) U-Pb geochronology of basement rocks in Central Tibet and paleogeographic implications.

Journal of Asian Earth Sciences **43**, 23–50. doi: 10.1016/j.jseaes.2011.09.003.

Halpin JA, Crawford AJ, Direen NG, Coffin MF, Forbes CJ and Borissova I (2008) Naturaliste Plateau, offshore Western Australia: a submarine window into Gondwana assembly and breakup. *Geology* **36**, 807–10. doi: 10.1130/G25059A.1.

Halpin JA, Jensen T, McGoldrick P, Meffre S, Berry RF, Everard JL, Calver CR, Thompson J, Goemann K and Whittaker JM (2014) Authigenic monazite and detrital zircon dating from the Proterozoic Rocky Cape Group, Tasmania: links to the Belt-Purcell Supergroup, North America. *Precambrian Research* **250**, 50–67. doi: 10.1016/j.precamres.2014.05.025.

Han YG, Zhao GC, Cawood PA, Sun M, Eizenhöfer PR, Hou WZ, Zhang XR and Liu Q (2016) Tarim and North China cratons linked to northern Gondwana through switching accretionary tectonics and collisional orogenesis. *Geology* **44**, 95–8. doi: 10.1130/G37399.1.

Harley SL, Fitzsimons IC and Zhao Y (2013) Antarctica and supercontinent evolution: historical perspectives, recent advances and unresolved issues. *Geological Society, London, Special Publications* **383**, 1–34. doi: 10.1144/SP383.9.

He HY, Wang YJ, Cawood PA, Qian X, Zhang YZ and Zhao GF (2020) Permo-Triassic granitoids, Hainan Island, link to Paleotethyan not Paleopacific tectonics. *Geological Society of America Bulletin* **132**, 2067–83. doi: 10.1130/B35370.1.

He HY, Wang YJ, Zhang YZ, Chen XY and Zhou YZ (2016) Extremely depleted Carboniferous N-MORB metabasites at the Chenxing area (Hainan) and its geological significance. *Earth Science* **41**, 1361–75 (in Chinese with English abstract). doi: 10.16539/j.ddgzyckx.2013.01.016.

Hoskin PWO and Schaltegger U (2003) The composition of zircon and igneous and metamorphic petrogenesis. *Reviews in Mineralogy and Geochemistry* **53**, 27–62. doi: 10.2113/0530027.

Hosseini SH, Sadeghian M, Zhai M and Ghasemi H (2015) Petrology, geochemistry and zircon U-Pb dating of Band-e-Hezarchah Metabasites (NE Iran): an evidence for back-arc magmatism along the Northern active margin of Gondwana. *Geochemistry* **75**, 207–18. doi: 10.1016/j.chemer.2015.02.002.

Hu N, Zhang RJ and Feng SN (2002) Study on Devonian-Carboniferous boundary in Hainan Island, South China. *Chinese Journal of Geology* **37**, 313–9. doi: 10.3321/j.issn:0563-5020.2002.03.007.

Kong JT, Xu ZJ and Cheng RH (2022) Detrital zircon geochronology of middle Paleozoic to lower Mesozoic strata from Hainan: implications for sedimentary provenance and tectonic evolution of Hainan. *International Journal of Earth Sciences* **111**, 2053–77. doi: 10.1007/s00531-022-02221-1.

Lee YI, Choi T, Lim HS and Orihashi Y (2016) Detrital zircon geochronology and Nd isotope geochemistry of the basal succession of the Taebaeksan Basin, South Korea: implications for the Gondwana linkage of the Sino-Korean (North China) block during the Neoproterozoic-early Cambrian. *Palaeogeography Palaeoclimatology Palaeoecology* **441**, 770–86. doi: 10.1016/j.palaeo.2015.10.025.

Leier AL, Kapp P, Gehrels GE and DeCelles PG (2007) Detrital zircon geochronology of Carboniferous-Cretaceous strata in the Lhasa Terrane, southern Tibet. *Basin Research* **19**, 361–78. doi: 10.1111/j.1365-2117.2007.00330. x.

Li GJ, Wang QF, Huang YH, Gao L and Li Y (2016) Petrogenesis of middle Ordovician peraluminous granites in the Baoshan block: implications for the early Paleozoic tectonic evolution along East Gondwana. *Lithos* **245**, 76–92. doi: 10.1016/j.lithos.2015.10.012.

Li SB, He HY, Qian X, Wang YJ and Zhang AM (2018) Carboniferous arc setting in Central Hainan: geochronological and geochemical evidences on the andesitic and dacitic rocks. *Journal of Earth Science* **29**, 265–79. doi: 10.1007/s12583-017-0936-0.

Li ZH, Fu TA, Zhang M, Xie CF, Peng SB and Chen HM (2007) Restudy on the Siliurian Llandovery Telychian stratigraphy of Nanhao area in Baoting County, Hainan Island. *South China Geology* **92**, 64–71. doi: 10.3969/j.issn.1007-3701.2007.04.010.

Li ZH, Zhou P, Peng ZQ, Cheng L and Wei YX (2009) Study of the Landovery Trlychian stratigraphical sequences in the Nanhao Area, Baoting country, Hainan Island. *Journal of Stratigraphy* **33**, 206–12. doi: 10.1016/S1874-8651(10)60080-4.

Li ZX, Li XH, Li WX and Ding S (2008) Was Cathaysia part of Proterozoic Larentia? –new data from Hainan Island, south China. *Terra Nova* **20**, 154–64. doi: 10.1111/j.1365-3121.2008.00802. x.

Li ZX, Li XH, Wartho JA, Clark C, Li WX, Zhang CL and Bao CM (2010) Magmatic and metamorphic events during the early Paleozoic Wuyi-Yunkai orogeny, southeastern South China: new age constraints and pressure–temperature conditions. *Geological Society of America Bulletin* **122**, 772–93. doi: org/10.1130/B30021.1.

Li ZX, Li XH, Zhou H and Kinny PD (2002) Grenvillian continental collision in south China: new SHRIMP U-Pb zircon results and implications for the configuration of Rodinia. *Geology* **30**, 163–6. doi: 10.1130/0091-7613(2002)030<0163: GCCISC>2.0.CO;2.

Link PK, Fanning CM, Lund KI and Aleinikoff JN (2007) Detrital zircons, correlation and provenance of Mesoproterozoic Belt Supergroup and correlative strata of east-central Idaho and southwest Montana. *Proterozoic Geology of Western North America and Siberia* **86**, 101–28. doi: 10.2110/pec.07.86.0101.

Liu GC (2020) Petrology component and geochronology of Early Paleozoic Proto-Tethys ophiolite mélange in SW Yunnan. China University of Geosciences. doi: 10.27492/d.cnki.gzdzu.2020.000029.

Liu GC, Sun ZB, Zeng WT, Feng QL, Huang L and Zhang H (2017) The age of Wanhe ophiolitic melange from Mengku area, Shuangjiang County, western Yunnnan Province, and its geological significance. *ACTA Petrologica et Mineralogica* **36**, 163–74. doi: 10.3969/j.issn.1000-6524.2017.02.003.

Liu H, Bi M, Guo X, Zhou Y and Wang Y (2019) Petrogenesis of Late Silurian volcanism in SW Yunnan (China) and implications of the tectonic reconstruction of northern Gondwana. *International Geology Review* **61**, 1297–312. doi: 10.1080/00206814.2018.1506947.

Liu H, Wang BD, Chen L, Huang F, Zeng YC and Wang LQ (2021) Silurian intermediate–felsic complex in the Xiangtaohu area of central Qiangtang, northern Tibet: evidence for southward subduction of the Longmuco–Shuanghu Prototethys oceanic plate. *Lithos* **404–405**, 1–15. doi: 10.1016/j.lithos.2021.106465.

Liu H, Xia X, Lai CK, Gan CS, Zhou YZ and Huangfu PP (2018) Break-away of South China from Gondwana: insights from the Silurian high-Nb basalts and associated magmatic rocks in the Diancangshan-Ailaoshan fold belt (SW China). *Lithos* **318**, 194–208. doi: 10.1016/j.lithos.2018.08.014.

Liu R, Zhou HW, Zhang L, Zhong ZQ, Zeng W, Xiang H, Jin S, Lu XQ and Li CZ (2010a) Zircon U–Pb ages and Hf isotope compositions of the Mayuan migmatite complex, NW Fujian Province, southeast China: constraints on the timing and nature of a regional tectonothermal event associated with the Caledonian orogeny. *Lithos* **119**, 163–80. doi: 10.1016/j.lithos.2010.06.004.

Liu XC, Hu J, Chen LY, Chen Y, Xia MM, Han JE and Hu DG (2022a) The Mulantou metamorphic complex from northeastern Hainan Island, South China: compositions, age and tectonic implications. *Acta Petrologica Sinica* **96**, 3051–83. doi: 10.1111/jmg.12563.

Liu YM, Li C, Xie CM, Fan JJ, Wu H, Jiang QY and Li X (2016) Cambrian granitic gneiss within the central Qiangtang terrane, Tibetan Plateau: implications for the Early Palaeozoic tectonic evolution of the Gondwanan margin. *International Geology Review* **58**, 1043–63. doi: 10.1080/00206814.2016.1141329.

Liu YM, Zhai QG, Hu PY, Tang Y and Lee HY (2022b) Evolution of the Paleo-Tethys Ocean: constraints from detrital zircons of the Paleozoic to Triassic clastic rocks in the Qiangtang terrane, Tibetan Plateau. *Journal of Asian Earth Sciences* **232**, 1–13. doi: 10.1016/j.jseaes.2022.105226.

Liu YS, Hu ZC, Zong KQ, Gao CG, Gao S, Xu J and Chen HH (2010b) Reappraisement and refinement of zircon U-Pb isotope and trace element analyses by LA-ICP-MS. *Chinese Science Bulletin* **55**, 1535–46.

Long WG, Tong JN, Zhu YH, Zhou JB, Li SX and Shi C (2007) Discovery of the Permian in the Danzhou-Tunchang area of Hainan Island and its geological significance. *Geology and Mineral Resources of South China* **1**, 38–45. doi: 10.3969/j.issn.1007-3701.2007.01.007.

Lu SN (2001) From Rodinia to Gondwanaland supercontinents—Thinking about problems of researching Neoproterozoic supercontinents. *Earth Science Frontiers* **8**, 441–8. doi: 10.3321/j.issn:1005-2321.2001.04.027.

Lu SN (2004) Comparison of the Pan-Cathaysian orogeny with the Caledonian and Pan-African orogenies. *Regional Geology of China* **23**, 952–8. doi: 10.3969/j.issn.1671-2552.2004.09.019.

Ludwig KR (2003) Isoplot 3.09–A geochronological toolkit for Microsoft Excel. *Berkeley Geochronology Center Special Publication*, 1–4.

Ma X, Yang KG and Polat A (2018) U–Pb ages and Hf isotopes of detrital zircons from pre-Devonian sequences along the southeast Yangtze: a link to the final assembly of East Gondwana. *Geological Magazine* **156**, 950–68. doi: 10.1017/S0016756818000511.

Malone DH, Craddock JP, Link PK, Foreman BZ, Scroggins MA and Rappe J (2017) Detrital zircon geochronology of quartzite clasts, northwest Wyoming: implications for Cordilleran Neoproterozoic stratigraphy and depositional patterns. *Precambrian Research* **289**, 116–28. doi: 10.1016/j.precamres.2016.12.011.

Malone SJ, Meert JG, Banerjee DM, Pandit MK, Tamrat E, Kamenov GD, Pradhan VR and Sohi LE (2008) Paleomagnetism and detrital zircongeochronology of the Upper Vindhyan sequence, Son Valley and Rajasthan, India: a ca. 1000 Ma closure age for the Purana Basins? *Precambrian Research* **164**, 137–59. doi: 10.1016/j.precamres.2008.04.004.

McKenzie NR, Hughes NC, Myrow PM, Banerjee DM, Deb M and Planavsky NJ (2013) New age constraints for the Proterozoic Aravalli-Delhi successions of India and their implications. *Precambrian Research* **238**, 120–28. doi: 10.1016/j.precamres.2013.10.006.

McKenzie NR, Hughes NC, Myrow PM, Xiao S and Sharma M (2011) Correlation of Precambrian–Cambrian sedimentary successions across northern India and the utility of isotopic signatures of Himalayan lithotectonic zones. *Earth and Planetary Science Letters* **312**, 471–83. doi: 10.1016/j.epsl.2011.10.027.

Meert JG (2003) A synopsis of events related to the assembly of eastern Gondwana. *Tectonophysics* **362**, 1–40. doi: 10.1016/S0040-1951(02)00629-7.

Meert JG and Lieberman BS (2008) The Neoproterozoic assembly of Gondwana and its relationship to the Ediacaran-Cambrian radiation. *Gondwana Research* **14**, 5–21. doi: 10.1016/j.gr.2007.06.007.

Metcalfe I (2011) Tectonic framework and Phanerozoic evolution of Sundaland. *Gondwana Research* **19**, 3–21. doi: 10.1016/j.gr.2010.02.016.

Metcalfe I (2013) Gondwana dispersion and Asian accretion: tectonic and palaeogeographic evolution of eastern Tethys. *Journal of Asian Earth Sciences* **66**, 1–33. doi: 10.1016/j.jseaes.2012.12.020.

Metcalfe I (2017) Tectonic evolution of Sundaland. *Bulletin of the Geological Society of Malaysia* **63**, 27–60. doi: 10.7186/bgsm63201702.

Miller C, Thoni M, Frank W, Grasemann B, Klotzli U, Guntli P and Draganits E (2001) The early Paleozoic magmatic event in the Northwest Himalaya, India: source, tectonic setting and age of emplacement. *Geological Magazine* **138**, 237–51. doi: 10.1016/j.gr.2007.06.007.

Mulder JA, Halpin JA and Daczko NR (2016) Mesoproterozoic Tasmania: witness to the East Antarctica–Laurentia connection within Nuna. *Geology* **44**, e383. doi: 10.1130/G37740Y.1.

Mulder JA, Karlstrom KE, Fletcher K, Heizler MT, Timmons JM, Crossey LJ, Gehrels GE and Pecha M (2017) The syn-orogenic sedimentary record of the Grenville Orogeny in southwest Laurentia. *Precambrian Research* **294**, 33–52. doi: 10.1016/j.precamres.2017.03.006.

Nakano N, Osanai Y, Owada M, Binh P, Hokada T, Kaiden H and Bui VTS (2021) Evolution of the Indochina block from its formation to amalgamation with Asia: constraints from protoliths in the Kontum Massif, Vietnam. *Gondwana Research* **90**, 47–62. doi: 10.1016/j.gr.2020.11.002.

Nguyen QM, Feng Q, Zi JW, Zhao T, Tran HT, Ngo TX, Tran DM and Nguyen HQ (2019) Cambrian intra-oceanic arc trondhjemite and tonalite in the Tam Ky-Phuoc Son Suture Zone, central Vietnam: implications for the early Paleozoic assembly of the Indochina Block. *Gondwana Research* **70**, 151–70. doi: 10.1016/j.gr.2019.01.002.

Nie XM (2016) Early-middle Paleozoic Tethyan evolution in SW Yunnan, China and Northern Thailand. China University of Geosciences.

Olieook HKH, Barham M, Fitzsimons ICW, Timms NE, Jiang Q, Evans NJ and McDonald BJ (2019) Tectonic controls on sediment provenance evolution in rift basins: detrital zircon U–Pb and Hf isotope analysis from the Perth Basin, Western Australia. *Gondwana Research* **66**, 126–42. doi: 10.1016/j.gr.2018.11.002.

Pankhurst RJ, Trouw RAJ, Brito Neves BB and Wit MJ (2008) West Gondwana: pre-cenozoic correlations across the South Atlantic region: London. *Geological Society* **294**, 681–2.

Peng H, Xie C, Li C and Zhang Z (2019) Provenance and palaeogeographic implications of detrital zircons from the lower Carboniferous Riwanchaka formation of the central Tibetan Plateau. *Geological Magazine* **156**, 2031–42. doi: 10.1017/S0016756819000359.

Peng ZM, Geng QR, Pan GT, Wang LQ, Zhang Z, Cong F and Guan JL (2014) Zircon SHRIMP geochronology and Nd-Pb isotopic characteristics of the meta-basalt in the Central Part of Tibetan Plateau's Qiangtang region. *Science China Earth Sciences* **57**, 428–38. doi: 10.1007/s11430-013-4693-3.

Peng ZM, Wang BD, Hu JF, Fu YZ, Wang GZ, Zhang J, Liu YH, Zhang Z, Guan JL and Han WW (2022) Determination and oceanic crust subduction of Early Palaeozoic accretionary complexes in the western Yunnnan Province—New cognition based on the geological survey of Wendong sheet (1∶50000). *Geology in China* **49**, 1656–72. (in Chinese with English abstract). doi: 10.12029/gc20220519.

Pisarevsky SA, Wingate MT, Powell CM, Johnson S and Evans DA (2003) Models of Rodinia assembly and fragmentation. *Geological Society* **206**, 35–55.

Powell CM, Jones D, Pisarevsky S and Wingate M (2001) Palaeomagnetic constraints on the position of the Kalahari craton in Rodinia. *Precambrian Research* **110**, 33–46.

Pullen A, Kapp P, Gehrels GE, Vervoort JD and Ding L (2008) Triassic continental subduction in central Tibet and Mediterranean-style closure of the Paleo-Tethys Ocean. *Geology*, **36**, 351–4. doi: 10.1130/G24435A.1.

Qi L, Cawood PA, Xu YJ, Du YS, Zhang HC and Zhang ZK (2020) Linking South China to North India from the late Tonian to Ediacaran: constraints from the Cathaysia Block. *Precambrian Research* **350**, 1–17. doi: 10.1016/j.precamres.2020.105898.

Rämö OT, McLemore T, Hamilton MA, Kosunen PJ, Heizler M and Haapala I (2003) Intermittent 1630–1220 Ma magmatism in central Mazatzal province: new geochronologic piercing points and some tectonic implications. *Geology* **31**, 335–8. doi: 10.1130/0091-7613(2003)031<0335:IMMICM>2.0.CO;2.

Ren P, Mou CL, Zhou G, Wang Q and Wang XP (2023) Provenance and tectonic settings of the Early Silurian clastic rocks in the southeast Upper Yangtze region: constraints from the whole-rock geochemistry and detrital zircon U–Pb geochronology. *Journal of Asian Earth Sciences* **250**, 1–20. doi: 10.1016/j.jseaes.2023.105644.

Replumaz A and Tapponnier P (2003) Reconstruction of the deformed collision zone between India and Asia by backward motion of lithospheric blocks. *Journal of Geophysical Research* **108**, 1–24. doi: 10.1029/2001JB000661.

Ross GM, Parrish RR and Dudas F (1991) Provenance of the Bonner formation (Belt Supergroup), Montana: insights from U–Pb and Sm-Nd analyses of detrital minerals. *Geology* **19**, 340–3. doi: 10.1130/0091-7613(1991)019<0340: POTBFB>2.3.CO;2.

Ross GM, Parrish RR and Winston D (1992) Provenance and U–Pb geochronology of the Mesoproterozoic Belt Supergroup (northwestern United States): implications for age of deposition and pre–Panthalassa plate reconstructions. *Earth and Planetary Science Letters* **113**, 57–76. doi: 10.1016/0012-821x (92)90211-d.

Ross GM and Villeneuve M (2003) Provenance of the Mesoproterozoic (1.45 Ga) Belt basin (western North America): another piece in the pre-Rodinia paleogeographic puzzle. *Geological Society of America Bulletin*, **115**, 1191–217. doi: 10.1130/B25209.1.

Rossetti F, Nozaem R, Lucci F, Vignaroli G, Gerdes A, Nasrabadi M and Theye T (2015) Tectonic setting and geochronology of the Cadomian (Ediacaran-Cambrian) magmatism in Central Iran, Kuh-e-Sarhangi Region (NW Lut Block). *Journal of Asian Earth Sciences* **102**, 24–44. doi: 10.1016/j.jseaes.2014.07.034.

Sajid M, Andersen J, Rocholl A and Wiedenbeck M (2018) U-Pb geochronology and petrogenesis of peraluminous granitoids from Northern Indian plate in NW Pakistan: Andean type orogenic signatures

from the Early Paleozoic along the Northern Gondwana. *Lithos* **318**, 340–56. doi: 10.1016/j.lithos.2018.08.024.

Satkoski AM, Wilkinson BH, Hietpas J and Samson SD (2013) Likeness among detrital zircon populations—An approach to the comparison of age frequency data in time and space. *Geological Society of America Bulletin* **125**, 1783–99. doi: 10.1130/b30888.1.

Saylor JE, Knowles JN, Horton BK, Nie JS and Mora A (2013) Mixing of source populations recorded in detrital zircon U-Pb age spectra of modern river sands. *The Journal of Geology* **121**, 17–33. doi: 10.1086/668683.

Saylor JE, Stockli DF, Horton BK and Nie JS (2012) Discriminating rapid exhumation from syndepositional volcanism using detrital zircon double dating: implications for the tectonic history of the Eastern Cordillera, Colombia. *Geological Society of America Bulletin* **124**, 762–79. doi: 10.1130/B30534.1.

Shi MF, Lin FC, Fan WY, Deng Q, Cong F, Tran MD, Zhu HP and Wang H (2015) Zircon U–Pb ages and geochemistry of granitoids in the Truong Son terrane, Vietnam: tectonic and metallogenic implications. *Journal of Asian Earth Sciences* **101**, 101–20. doi: 10.1016/j.jseaes.2015.02.001.

Sláma J, Kosler J, Condon DJ, Crowley JL, Gerdes A, Hanchar JM, Horstwood MSA, Morris GA, Nasdala L, Norberg N, Schaltegger U, Schoene B, Tubrett MN and Whitehouse MJ (2008) Plešovice zircon—A new natural reference material for U–Pb and Hf isotopic microanalysis. *Chemical Geology* **249**, 1–35.

Sorkhabi R and Heydari E (2008) Asia out of Tethys: foreword. *Tectonophysics* **451**, 1–6. doi: 10.1016/j.tecto.2007.11.043.

Stewart ED, Link PK, Fanning CM, Frost CD and McCurry M (2010) Paleogeographic implications of non-North American sediment in the Mesoproterozoic upper Belt Supergroup and Lemhi group, Idaho and Montana, USA. *Geology* **38**, 927–30. doi: 10.1130/g31194.1.

Sun SS and McDonough WF (1989) Chemical and isotopic systematics of oceanic basalts: implications for mantle composition and processes. *Geological Society*, **42**, 313–45. https://doi.org/10.1144/GSL.SP.1989.042.01.19.

Suzuki K, Kurihara T, Sato T, Ueda H, Takahashi T, Wilde SA and Satish-Kumar K (2023) Detrital zircon U–Pb ages and geochemistry of Devonian–Carboniferous sandstones and volcanic rocks of the Hida Gaien belt, Southwest Japan: provenance reveals a Gondwanan lineage for the early Paleozoic tectonic evolution of proto-Japan. *Gondwana Research* **115**, 224–55. doi: 10.1016/j.gr.2022.12.005.

Tang LM (2010) Magmatic evidence of two tectonic extension events during the Mesozoic in Hainan Island & geodynamic implications, Zhejiang University.

Tang M, Chu X, Hao J and Shen B (2021) Orogenic quiescence in Earth's middle age. *Science* **371**, 728–31. doi: 10.1126/science.abf1876.

Tang M, Ji WQ, Chu X,Wu AB and Chen C (2020) Reconstructing crustal thickness evolution from europium anomalies in detrital zircons. *Geology* **49**, 76–80. doi: 10.1130/G47745.1.

Tran HT, Zaw K, Halpin JA, Manaka T, Meffre S, Lai CK, Lee Y, Le HV and Dinh S (2014) The Tam Ky-Phuoc Son Shear Zone in central Vietnam: tectonic and metallogenic implications. *Gondwana Research* **26**, 144–64. doi: 10.1016/j.gr.2013.04.008.

Turner CC, Meert JG, Pandit MK and Kamenov GD (2014) A detrital zircon U–Pb and Hf isotopic transect across the Son Valley sector of the Vindhyan Basin, India: implications for basin evolution and Paleogeography. *Gondwana Research* **26**, 348–64. doi: 10.1016/j.gr.2013.07.009.

Usuki T, Lan CY, Wang KL and Chiu HY (2013) Linking the Indochina block and Gondwana during the Early Paleozoic: evidence from U–Pb ages and Hf isotopes of detrital zircons. *Tectonophysics* **586**, 145–59. doi: 10.1016/j.tecto.2012.11.010.

Veevers JJ, Saeed A, Belousova EA and Griffin WL (2005) U–Pb ages and source composition by Hf-isotope and trace-element analysis of detrital zircons in Permian sandstone and modern sand from southwestern Australia and a review of the paleogeographical and denudational history of the Yilgarn Craton. *Earth-Science Reviews* **68**, 245–79. doi: 10.1016/j.earscirev.2004.05.005.

Vermeesch P (2012) On the visualisation of detrital age distributions. *Chemical Geology* **312–313**, 190–194. doi: 10.1016/j.chemgeo.2012.04.021.

Vermeesch P (2013) Multi-sample comparison of detrital age distributions. *Chemical Geology* **341**, 140–6. doi: 10.1016/j.chemgeo.2013.01.010.

Wang BD, Wang LQ, Pan GT, Yin FG, Wang DB and Tang Y (2013a) U–Pb zircon dating of early Paleozoic gabbro from the Nantinghe ophiolite in the Changning–Menglian suture zone and its geological implication. *Chinese Science Bulletin* **58**, 920–30. doi: 10.1007/s11434-012-5481-8.

Wang BD, Wang LQ, Pan GT, Yin FG, Wang DB and Tang Y (2013b) U-Pb zircon dating of Early Paleozoic gabbro from the Nantinghe ophiolite in the Changning-Menglian suture zone and its geological implication. *China Science Bulletin* **58**, 344–54.

Wang C, Liang X, Foster DA, Fu JG, Jiang Y, Dong CG, Zhou Y, Wen SN and Quynh PV (2016) Detrital zircon U–Pb geochronology, Lu–Hf isotopes and REE geochemistry constrains on the provenance and tectonic setting of Indochina Block in the Paleozoic. *Tectonophysics* **677–678**, 125–34. doi: 10.1016/j.tecto.2016.04.008.

Wang C, Wei CX, Yun P, Lv CY, Lv ZY and Meng ZY (2019) Zircon U-Pb age, geochemistry and geological significance of Shunzuo granite in Wuzhishan area, Hainan Island. *Geological Bulletin of China* **38**, 1352–61. doi: 10.12097/j.issn.1671-2552.2019.08.011.

Wang HT, Zhai QG, Hu PY, Zeng LS, Tang Y and Zhu ZC (2020) Late Cambrian to Early Silurian granitic rocks of the Gemuri area, Central Qiangtang, North Tibet: new constraints on the tectonic evolution of the Northern Margin of Gondwana. *ACTA Geological Sinica* **94**, 1007–19. doi: 10.1111/1755-6724.14556.

Wang Q, Zhu DC, Cawood PA, Chung SL and Zhao ZD (2021c) Resolving the paleogeographic puzzle of the Lhasa Terrane in Southern Tibet. *Geophysical Research Letters* **48**, e2021GL094236. doi: 10.1029/2021GL094236.

Wang XF, Ma DQ and Jiang DH (1992) Geology of Hainan Island (1)-stratigraphic paleontology: Geological Publishing House, Beijing, 1–103.

Wang YJ, Zhang FF, Fan WM, Zhang GW, Chen SY, Cawood PA and Zhang AM (2010) Tectonic setting of the South China Block in the early Paleozoic: resolving intracontinental and ocean closure models from detrital zircon U–Pb geochronology. *Tectonics* **29**, 1–16. doi: 10.1029/2010TC002750.

Wang YJ, Zhang YZ, Qian X, Seneboutalath V, Wang Y, Wang YK, Gan CS and Zaw K (2021b) Ordo-Silurian assemblage in the Indochina interior: geochronological, elemental, and Sr-Nd-Pb-Hf-O isotopic constraints of Early Paleozoic Granitoids in South Laos. *Geological Society of America Bulletin* **133**, 325–346. doi: 10.1130/b35605.1.

Wang YJ., Zhang YZ, Qian X, Wang Y, Cawood PA, Gan CS and Seneboutalath V (2021a) Early Paleozoic accretionary orogenesis in the northeastern Indochina and implications for the paleogeography of East Gondwana: constraints from igneous and sedimentary rocks. *Lithos* **382–383**, 1–19. doi: 10.1016/j.lithos.2020.105921.

Wen SN, Liang XQ, Fan WM, Wang YJ, Chi GX, Liang XR, Zhou Y and Jiang Y (2013) Zircon U-Pb ages, Hf isotopic composition of Zhizhong granitic intrusion in Ledong area of Hainan Island and their tectonic implications. *Geotectonica et Metallogenia* **37**, 294–307. doi: 10.16539/j.ddgzyckx.2013.02.014.

Wiedenbeck MAPC, Alle P, Corfu FY, Griffin WL, Meier M, Oberli F, Von Quadt A, Roddick JC and Spiegel W (1995) Three natural zircon standards for U-Th-Pb, Lu-Hf, trace element and REE analyses. *Geostandards Newsletter* **19**, 1–23. https://doi.org/10.1111/j.1751-908X.1995.tb00147.x.

Wissink GK, Wilkinson BH and Hoke GD (2018) Pairwise sample comparisons and multidimensional scaling of detrital zircon ages with examples from the North American platform, basin, and passive margin settings. *Lithosphere* **10**, 478–91. doi: 10.1130/l700.1.

Wu GH, Chu X, Tang M, Li WY and Chen FK (2023) Distinct tectono-magmatism on the margins of Rodinia and Gondwana. *Earth and Planetary Science Letters* **609**, 1–9. doi: 10.1016/j.epsl.2023.118099.

Wu Y and Zheng Y (2004) Genesis of zircon and its constraints on interpretation of U–Pb age. *Chinese Science Bulletin* **49**, 1554–69. doi: 10.1360/04wd0130.

Xia XP, Nie XS and Lai CK (2016) Where was the Ailaoshan Ocean and when did it open: a perspective based on detrital zircon U–Pb age and Hf isotope evidence. *Gondwana Research* **36**, 488–502. doi: 10.1016/j.gr.2015.08.006.

Xia Y, Xu XS, Zhou HB and Liu L (2014) Early Paleozoic crust–mantle interaction and lithosphere delamination in South China Block: evidence

from geochronology, geochemistry, and Sr–Nd–Hf isotopes of granites. *Lithos* **184**, 416–35. doi: 10.1016/j.lithos.2013.11.014.

Xing XW (2016) Early Paleozoic tectonic nature in SW Yunnan: constraints from magmatism and sedimentation, University of Chinese Academy of Sciences.

Xu YJ, Cawood PA, Du Y, Zhong Z and Hughes NC (2014) Terminal suturing of Gondwana along the southern margin of South China Craton: evidence from detrital zircon U-Pb ages and Hf isotopes in Cambrian and Ordovician strata, Hainan Island. *Tectonics* **32**, 2490–504. doi: 10.1002/2014TC003748.

Xu YJ, Cawood PA, Du YS, Hu LS, Yu WC, Zhu YH and Li WC (2013) Linking south China to northern Australia and India on the margin of Gondwana: constraints from detrital zircon U-Pb and Hf isotopes in Cambrian strata. *Tectonics* **32**, 1547–58. doi: 10.1002/tect.20099.

Xu YJ, Cawood PA, Zhang HC, Zi JW, Zhou JB, Li LX and Du YS (2019) The Mesoproterozoic Baoban complex, South China: a missing fragment of western Laurentian lithosphere. *The Geological Society of America Bulletin* **132**, 1404–18. doi: 10.1130/B35380.1.

Xu YJ, Du YS, Cawood PA, Zhu YH, Li WC and Yu WC (2012) Detrital zircon provenance of upper Ordovician and Silurian strata in the northeastern Yangtze Block: response to orogenesis in South China. *Sedimentary Geology* **267**, 63–72. doi: 10.1016/j.sedgeo.2012.05.009.

Xu ZQ, Yang JS, Li HQ, Wang RR and Cai ZH (2012) Indosinian collision-orogenic system of Chinese continent and its orogenic mechanism. *Acta Petrologica Sinic*, **28**, 1697–709.

Xu ZQ, Yang JS, Liang FH, Qi XX, Zeng LS, Liu MY, Li HB, Wu CL, Shi RD and Chen SY (2005) Pan-African and Early Paleozoic orogenic events in the Himalaya terrane: inference from SHRIMP U-Pb zircon ages. *Acta Petrologica Sinica* **21**, 1–12. doi: 10.3321/j.issn:1000-0569.2005.01.001.

Yan QS, Metcalfe I and Shi XF (2017) U-Pb isotope geochronology and geochemistry of granites from Hainan Island (northern South China Sea margin): constraints on late Paleozoic-Mesozoic tectonic evolution. *Gondwana Research* **49**, 333–49. doi: 10.1016/j.gr.2017.06.007.

Yang JH, Cawood PA, Du YS, Huang H and Hu L (2012a) Large Igneous Province and magmatic arc sourced Permian-Triassic volcanogenic sediments in China. *Sedimentary Geology* **261**, 120–31. doi: 10.1016/j.sedgeo.2012.03.018.

Yang JH, Cawood PA, Du YS, Huang H and Hu L (2012b) Detrital record of Indosinian mountain building in SW China: Provenance of the Middle Triassic turbidites in the Youjiang Basin. *Tectonophysics* **574**, 105–17. doi: 10.1016/j.tecto.2012.08.027.

Yang XJ, Jia XC, Xiong CL, Bai XZ, Huang BX, Luo G and Yang CB (2012c) LA-ICP-MS zircon U-Pb age of metamorphic basic volcanic rock in Gongyanghe group of southern Gaoligong Mountain, western Yunnan Province, and its geological significance. *Geological Bulletin of China* **31**, 264–76. doi: 10.3969/j.issn.1671-2552.2012.02.009.

Yao HZ, Huang ZX, Xie CF and Zhang KM (1999) The Cambrian lithostratigraphical sequence and sedimentary facies of Wanning Area, Hainan Island. *Journal of Stratigraphy* **23**, 270–76. doi: 10.19839/j.cnki.dcxzz.1999.04.005.

Yao HZ, Zhang RJ, Niu ZJ, Tu B, Wang ZH, He YY, Song F, Zhao LS, Wang JX, Wang Y and Long WG (2021) Frasnian–Tournaisian (Late Devonian to Earliest Carboniferous) lithostratigraphy and biostratigraphy of Hainan Island, South China. *Geological Journal* **56**, 5987–99. doi: 10.1002/gj.4112.

Yao JL, Shu LS and Santosh M (2011) Detrital zircon U–Pb geochronology, Hf–sotopes and geochemistry: new clues for the Precambrian crustal evolution of Cathaysia Block, South China. *Gondwana Research* **20**, 553–67. doi: 10.1016/j.gr.2011.01.005.

Yao WH, Li ZX, Li WX and Li XH (2017) Proterozoic tectonics of Hainan Island in supercontinent cycles: new insights from geochronological and isotopic results. *Precambrian Research* **290**, 86–100. doi: 10.1016/j.precamres.2017.01.001.

Yuan HL, Gao S, Liu XM, Günther D and Wu FY (2004) Accurate U-Pb age and trace element determinations of zircon by laser ablation-inductively coupled plasma-mass spectrometry. *Geostandards and Geoanalytical Research* **28**, 353–70. doi: 10.1111/j.1751-908X.2004.tb00755. x.

Zeng QL, Li ZH, Xie CF, Fu TA and Zhang M (2003) On the Silurian strata of the Hainan Island area, China. *Journal of Stratigraphy* **27**, 267–75. doi: 10.3969/j.issn.0253-4959.2003.04.001.

Zeng QL, Li ZH, Xie CF, Fu TA and Zhang M (2004) Discovery of late Liand overian Brachiopod *Xinanospirifer* from Hainan Island Area, China with comments on the Nanhao Formation. *Acta Palaeontologica* **43**, 86–93. doi: 10.3969/j.issn.0001-6616.2004.01.008.

Zhang HC, Xu YJ, Cawood PA, Zhang YH and Du YS (2022) Ordovician amphibolite-facies metamorphism in Hainan Island: a record of early Paleozoic accretionary orogenesis along the northern margin of East Gondwana? *Journal of Asian Earth Sciences* **229**, 1–18. doi: 10.1016/j.jseaes.2022.105161.

Zhang HC, Xu YJ, Cawood PA, Zi JW, Zhou JB and Du YS (2023) Linking the Paleozoic evolution of Hainan Island to Indochina and Australia: implication for the paleogeography of the Eastern Tethys Ocean. *Tectonophysics* **858**, 1–16. doi: 10.1016/j.tecto.2023.229882.

Zhang HM (1994) Supercontinent and supercontinent cycle, Gondwana composition and Tethys evolution. *Overseas Precambrian Geology* **4**, 61–70.

Zhang L, Wang P, Chen XY and Yin Y (2020a) Review in detrital zircon U-Pb geochronology: data acquisition, analysis and comparison. *Advances in Earth Science* **35**, 414–30. doi: 10.15898/j.cnki.11-2131/td.202112260209.

Zhang LM, Cawood PA, Wang YJ, Cui X, Zhang YZ, Qian X and Zhang FF (2020b) Provenance record of late Mesoproterozoic to Early Neoproterozoic Units, West Hainan, South China, and implications for Rodinia reconstruction. *Tectonic* **39**, 1–19. doi: 10.1029/2020TC006071.

Zhang LM, Wang YJ, Qian X, Zhang YZ, He HY and Zhang AM (2018a) Petrogenesis of Mesoproterozoic mafic rocks in Hainan (South China) and its implication on the Southwest Hainan-Laurentia-Australia connection. *Precambrian Research* **313**, 119–33. doi: 10.1016/j.precamres.2018.05.002.

Zhang LM, Wang YJ, Zhang YZ, Liu HC and Zhang XC (2017) Age of paleozoic strata in Northern Hainan Island: constraints from the detrital zircon U-Pb geochronology. *Journal of Jilin University (Earth Science Edition)* **47**, 1187–206. doi: 10.13278/j.cnki.jjuese.201704116.

Zhang LM, Zhang YZ, Cui X, Cawood PA, Wang YJ and Zhang AM (2019) Mesoproterozoic rift setting of SW Hainan: evidence from the gneissic granites and metasedimentary rocks. *Precambrian Research* **325**, 69–87. doi: 10.1016/j.precamres.2019.02.013.

Zhang Q, Jiang YH, Wang GC, Liu Z, Ni CY and Qing L (2015) Origin of Silurian gabbros and I-type granites in central Fujian, SE China: implications for the evolution of the early Palezoic orogen of South China. *Lithos* **216–217**, 285–97. doi: 10.1016/j.lithos.2015.01.002.

Zhang RJ, Tu B and Zeng BF (2013) Re-discussion on the geological age of "Nanhao Formation" in Nanhao area, Hainan Island—With comments on the paper "Geological characters and age of Nanhao Formation, Nanhao area, Hainan Province". *Geology in China* **40**, 1180–8. doi: 10.3969/j.issn.1000-3657.2013.04.016.

Zhang XR, Chung SL, Lai YM, Ghani AA, Murtadha S, Lee HY and Hsu CC (2018b) Detrital zircons dismember Sibumasu in East Gondwana. *Journal of Geophysical Research: Solid Earth* **123**, 6098–110. doi: 10.1029/2018JB015780.

Zhang XZ, Dong YS, Li C, Deng MR, Zhang L and Xu W (2014) Silurian high-pressure granulites from Central Qiangtang, Tibet: constraints on early Paleozoic collision along the northeastern margin of Gondwana. *Earth and Planetary Science Letters* **405**, 39–51. doi: 10.1016/j.epsl.2014.08.013.

Zhang YM, Xie CF, Fu TA and Li ZH (2005) Tectonic evolution of Hainan Island. *Science Technology and Engineering* **5**, 1485–7. doi: 10.3969/j.issn.1671-1815.2005.20.005.

Zhao GC, Wang YJ, Huang B, Dong YP, Li SZ, Zhang GW and Yu S (2018) Geological reconstructions of the East Asian blocks: from the breakup of Rodinia to the assembly of Pangea. *Earth-Science Reviews* **186**, 262–86. doi: 10.1016/j.earscirev.2018.10.003.

Zhao SW, Lai SC, Qin JF and Zhu RZ (2016) Tectono-magmatic evolution of the Gaoligong Belt, Southeastern margin of the Tibetan Plateau: constraints from granitic gneisses and granitoid intrusions. *Gondwana Research* **35**, 238–56. doi: 10.1016/j.gr.2015.05.007.

Zhao TY (2019) Early Paleozoic Proto-Tethys tectonic evolution in SW Yunnan: constraints from detrital zircon U-Pb geochronology and granite associations. China University of Geosciences. doi: 10.27492/d.cnki.gzdzu.2019.000275.

Zhao TY, Feng QL, Metcalfe I, Milan LA, Liu GC and Zhang ZB (2017) Detrital zircon U-Pb-Hf isotopes and provenance of Late Neoproterozoic

and Early Paleozoic sediments of the Simao and Baoshan blocks, SW China: implications for Proto-Tethys and Paleo-Tethys evolution and Gondwana reconstruction. *Gondwana Research* **51**, 193–208. doi: 10.1016/j.gr.2017.07.012.

Zhao XM, Hu ZL, Pei YJ, Yuan HJ, Qiu XF, Wu NW and Yao HZ (2021) Recognition of metamorphic conglomerate in the Sanya area of Hainan Island and its indicator to breakup of the Columbia supercontinent. *Geological Bulletin of China* **40**, 880–88.

Zhao XM, Yao HZ, Pei YJ, Hu ZL, Yuan HJ, Wang Y, Zhang RJ, He JL, Long WG and Wu NW (2020) The discovery of Devonian strata in Lanyang area, Danzhou, Hainan Province: evidence from the zircon U-Pb ages. *Geological Bulletin of China* **39**, 818–26. doi: 10.12097/j.issn.1671-2552.2020.06.003.

Zhou ML, Xia XP, Peng TP, Xu J and Ma PF (2020) etrital zircon U-Pb-Hf isotope studies for the Paleozoic sandstones from the Baoshan Block, western Yunnan, and their constraints on the Gondwana continental reconstruction. *Acta Petrologica Sinica* **36**, 469–83. doi: 10.18654/1000-0569/2020.02.09.

Zhou XY (2018) Compositions of the Neoproterozoic to early Paleozoic basement rocks and its tectonic significance, in Southeast Yunnan-North Vietnam. Nanjing University. doi: 10.27235/d.cnki.gnjiu.2018.000327.

Zhou Y, Liang XQ, Liang XR, Jiang Y, Wang C, Fu JG and Shao TB (2015a) U–Pb geochronology and Hf–isotopes on detrital zircons of Lower Paleozoic strata from Hainan Island: new clues for the early crustal evolution of southeastern South China. *Gondwana Research* **27**, 1586–98. doi: 10.1016/j.gr.2014.01.015.

Zhou Y, Liang XQ, Liang XR, Jiang Y, Zou SC, Wang C, Fu JG and Dong CG (2015b) Geochronology and geochemistry of cretaceous volcanic rocks from Liuluo formation in Hainan Island and their tectonic implications. *Geotectonica et Metallogenia* **39**, 903–18. doi: 10.16539/j.ddgzyckx.2015.05.013.

Zhou Y, Sun SY, Feng ZH, Xu C, Cai YF, Liang XQ, Liu XJ and Du YJ (2021a) A new insight into the Eastern extension of the Proto-Tethyan margin of Gondwana by early Paleozoic volcanic rocks in South China. *Lithos* **398–399**, 1–12. doi: 10.1016/j.lithos.2021.106328.

Zhou Y, Zhao YS, Du YJ, Cai YF, Feng ZM, Liu XJ and Song HX (2021b) Identification of Early Paleozoic Andesite in Northwestern Hainan Island and its geotectonic significances. *Earth Science* **46**, 3850–60.

Zhu DC, Zhao ZD, Niu Y, Dilek Y and Mo XX (2011) Lhasa terrane in southern Tibet came from Australia. *Geology* **39**, 727–30. doi: 10.1130/G31895.1.

Zhu DC, Zhao ZD, Niu YL, Dilek Y, Wang Q, Ji WH, Dong GC, Sui QL, Liu YS, Yuan HL and Mo XX (2012) Cambrian bimodal volcanism in the Lhasa Terrane, Southern Tibet: record of an Early Paleozoic Andean-type magmatic arc in the Australian proto-Tethyan margin. *Chemical Geology* **328**, 290–308. doi: 10.1016/j.chemgeo.2011.12.024.